



Cite this: *Green Chem.*, 2024, **26**, 720

## Adsorptive separation of saccharides and polyols over materials functionalized with boronate groups

Irina Delidovich \* and Valérie Toussaint

Saccharides and polyols play key roles in emerging biomass-based value chains, though recovery of these compounds from product streams remains challenging. This Review addresses the application of materials bearing boronate groups for separation and recovery of saccharides and polyols *via* affinity adsorption processes. First, the representative, industrially important product mixtures are considered, along with the design of separation processes exploiting the affinity adsorption. Thereafter, the structure-performance correlations are critically discussed for gel-type functionalized polymers, macroporous resins, molecularly imprinted polymers, and materials bearing grafted phenylboronate moieties and grafted polymer brushes. Finally, the separation processes based on functional materials bearing boronate groups are compared with the state-of-the-art chromatographic separation over  $\text{Ca}^{2+}$  ion-exchange resins. This analysis aims at identifying guidelines for rational material synthesis and knowledge-driven process design for novel economically viable and environmentally benign separation processes.

Received 23rd October 2023,  
Accepted 11th December 2023

DOI: 10.1039/d3gc04049f

rsc.li/greenchem

### 1. Motivation

Transition from exhaustible fossil resources to renewable feedstocks presents a key aspect of sustainable development. Lignocellulose is not digestible by humans and belongs thus to biomass sources of the second generation. Lignocellulose is available as a component of waste streams in forestry, agriculture, paper, and pulp production. On average, a cell wall consists of 35–50% cellulose, 20–40% hemicelluloses, 5–30% lignin, and 1–10% other extracted substrates.<sup>1</sup> An interest in lignocellulose as industrial organic raw material is caused by its abundance, availability from waste streams, and high carbohydrate content of 60–70%.

Comparison of typical naphtha components, mainly represented by linear alkanes  $\text{C}_n\text{H}_{2n+2}$ , with lignocellulose of an average formula  $\text{C}_3\text{H}_4\text{O}_2$ ,<sup>2</sup> suggests significant differences in chemical structures, physical and chemical properties of the fossil and bio raw materials. Transformation of alkanes into custom products requires functionalization, whereas biomass-based raw materials and intermediates frequently require rather de-functionalization than functionalization.<sup>3</sup> These compounds contain high content of oxygen, exhibit high boiling points, low vapor pressures, and/or decompose upon heating. A simple and energy-efficient integration of biomass

into existing value chains to produce conventional base chemicals and intermediates poses a challenge.

A complete re-design of the value chains upon the shift from naphtha to biomass feedstocks presents an alternative for an integration into the existing value chains. A concept of converting sugars into fuels and chemicals *via* novel 12 “building block chemicals” rather than conventional base chemicals was proposed by the US Department of Energy (DoE) in 2004.<sup>4</sup> In 2010, this list was revisited, and only 10 “building block chemicals”, which are also referred to as “platform chemicals”, were proposed (Fig. 1).<sup>5</sup> This approach combines depolymerization of the complex biomass-derived polymers and selective defunctionalization of the obtained monomers into novel platform chemicals.<sup>4–15</sup> High density of the functional groups available in the platform molecules opens numerous possibilities for tailored chemical transformations.<sup>16</sup>

Remarkably, separation and purification costs account for the major production and operating costs in biorefineries. Robust separation technologies are therefore critical to have biomass-based industry economically viable.<sup>17</sup> Diluted and complex product streams are responsible for costly separations in biorefineries. Liquid crude oil, which is currently used as the main feedstock in industry, requires no dilution for processing. In contrast, pulp mill receives a feedstock that is solid and consists out of 50% water. To process the fiber into desired products, size reduction, and further dilution are required. Finally, multi-component streams containing the target product in the concentration range of 1–5 wt% are

*Institute of Chemical, Environmental and Bioscience Engineering, TU Wien, Getreidemarkt 9, 1060 Vienna, Austria. E-mail: irina.delidovich@tuwien.ac.at*





Fig. 1 Structures of ten molecules indicated by DoE as platform chemicals.<sup>5</sup>

obtained. High dilution rates result in high recovery costs, which are usually inversely proportional to the product concentration in streams.<sup>18</sup> The products and intermediates in biorefineries frequently exhibit high polarity, high boiling points along with low thermal stability. Consequently, application of conventional separation methods, such as distillation<sup>19,20</sup> or liquid–liquid extraction,<sup>21</sup> is either impossible or not economically feasible.

This Review Article focuses on recovery of sugar alcohols and saccharides from product streams in biorefineries. Section 2 addresses the role of saccharides and sugar alcohols in novel value chains. Processes which are based on adsorptive uptake of materials bearing boronate moieties are considered in section 3. Advances in preparation of adsorbents with boronate functionalities are summarized in section 4. Finally,

section 5 provides a critical comparison of the currently used chromatographic separation over  $\text{Ca}^{2+}$  ion-exchange resins with adsorptive separation exploiting boronate-bearing materials and lists further steps which would facilitate application of adsorbents with boronate functionalities for separation in biorefineries.

## 2. Polyols and saccharides as elements of value chains

The current list of DoE “building block chemicals” contains three polyols, namely glycerol, D-sorbitol, and D-xylitol (Fig. 1).

- Glycerol is a co-product of fatty acid methyl ester (FAME) obtained as crude glycerol, a solution containing water and salts. Costly vacuum distillation is the state-of-the-art separation technology commercially used for purification of glycerol.<sup>22,23</sup>

- Starch is used as a raw material for production of D-sorbitol. First, starch is enzymatically hydrolyzed to yield D-glucose, which is further hydrogenated in the presence of a Ni catalyst. Purification of D-sorbitol includes numerous stages of treatment with ion-exchange resins to perform desalination.<sup>24</sup>

- Production of D-xylitol resembles the production of D-sorbitol: D-xylose is obtained from hydrolysates of hemicelluloses and is catalytically hydrogenated in the presence of Ni.<sup>24</sup> Strikingly, D-xylitol is significantly more costly than D-sorbitol, *i.e.* their prices were estimated as 3900 \$ per ton *vs.* 650 \$ per ton, respectively.<sup>25</sup> Hemicelluloses present heteropolymers, whose hydrolysis results in a number of monosaccharides: D-xylose, D-galactose, L-arabinose, D-glucose, and D-mannose as well as glucuronic acid and acetic acids.<sup>26</sup> Two alternatives to produce D-xylitol are possible: either the monosaccharides are separated to isolate D-xylose prior to hydrogenation or a



Irina Delidovich (right) and Valérie Toussaint (left)

Irina Delidovich is an Assistant Professor of Sustainable Use of Natural Resources at the TU Wien. She received her diploma in chemistry in 2008 from the Novosibirsk State University. In 2011, she obtained her Ph.D. degree from the Boreskov Institute of

Catalysis under the supervision of Prof. O. Taran. In 2012, she joined the research group of Prof. R. Palkovits at the RWTH Aachen University to conduct studies on the conversion of cellulosic biomass. Her scientific interests include catalytic transformations of saccharides as well as efficient separation methods in biorefining.

Valérie Toussaint obtained her diploma in chemistry in 2021 from the RWTH Aachen University (Aachen, Germany). In 2021, she started her Ph.D. in the field of technical chemistry at TU Wien (Vienna, Austria), working together with Assistant Prof. Irina Delidovich. Her research interests include synthesis and characterisation of heterogeneous catalysts for isomerization and epimerization of monosaccharides. As the development of an efficient product recovery presents a key element of process design, her research also addresses product separation via adsorption, focusing on elaborating materials with high affinity towards the desired products.



mixture of the hemicellulosic monosaccharides is hydrogenated and the obtained sugar alcohols are thereafter separated to yield pure *D*-xylitol. These chromatographically performed separations are mainly responsible for a high price of *D*-xylitol.<sup>25</sup>

Noteworthy, potentially industrially relevant polyols are not limited to the platform chemicals designated by DoE. Further examples of commercially relevant saccharides and sugar alcohols, whose separation presents a bottleneck of the process, are known. For instance, biotechnologically produced 2,3-butanediol<sup>27,28</sup> or ethylene glycol and propylene glycol<sup>29</sup> as products of hydrogenolysis can hardly be recovered from the obtained aqueous product streams.

Separation of monosaccharides as intermediates for production of platform chemicals is another important challenge. For example, commercial production of furanics as versatile platform molecules requires certain saccharide substrates dissolved in an appropriate solvent in a high concentration. Numerous attempts to develop a profitable method for synthesis of 5-(hydroxymethyl)furfural (HMF) have been undertaken. Acid-catalyzed dehydration of *D*-glucose and *D*-fructose in water as solvent results in 10%<sup>30</sup> and 50%<sup>31,32</sup> yields of HMF, respectively. A method for acid-catalyzed rehydration of *D*-fructose to obtain a mixture of HMF and 5-(methoxymethyl)furfural (MMF) in up to 70% combined yield using methanol as a solvent was recently developed. Application of methanol instead of water results in suppression of HMF dehydration into levulinic acid and formic acid.<sup>33</sup>

Avantium explored *D*-fructose-based production of MMF and HMF as well as selective oxidation of these molecules to produce 2,5-furandicarboxylic acid (FDCA) on a pilot plant scale. Moreover, Avantium provided promising results for polymerization of FDCA with ethylene glycol – the latter is already available on an industrial scale based on bioethanol<sup>25</sup> – to obtain polyethylene 2,5-furandicarboxylate (PEF), a polyester suitable for packaging, fibers, and films (Fig. 2). Recently, an upscaling to Flagship Plant based on *D*-fructose as a starting material was announced by Avantium.<sup>34</sup>

*D*-Fructose is produced nowadays as a part of high fructose corn syrup (HFCS; 42–55% fructose, rest glucose, and 1–4% oligosaccharides), a liquid alternative sweetener to sucrose made from corn. This is by far the largest synthetic biocatalytic process.<sup>35</sup> The major applications of HFCS are now carbonated beverages and raised bakery products.<sup>36</sup> Starch is nowadays used as a starting material for production of HFCS. Comparing the scales of polyester production – 24.23 Mt polyethylene terephthalate (PET) were produced in 2021 – with the available supply of 14 Mt of HFCS, it becomes obvious that an increase in demand of *D*-fructose is expected in the near future.

Profitable conversion of hemicellulosic pentoses (*D*-xylose and *L*-arabinose) into furfural shown in Fig. 3 presents another difficult task. Acid pre-treatment of lignocellulose results in highly diluted streams of hemicellulosic saccharides, whose concentration typically does not exceed 2 wt%. Economically efficient separation and concentration of saccharides from hydrolysates of hemicelluloses poses another challenge.<sup>37</sup>

Currently, saccharides are not recovered from industrial streams, with a few exceptions for separation of value-added products, such as *D*-fructose or *L*-arabinose. For instance, molasses consist of concentrated aqueous sugar solutions – sucrose and sometimes invert sugar – available as by-products at sugar mills. Molasses are composed of up to 50% of sugars and up to 17% of dissolved salts and are used without separation as animal feed or feedstock for fermentation.<sup>38</sup> Stepwise



Fig. 3 Conversion of *D*-xylose and *L*-arabinose into furfural.



Fig. 2 A production chain of polyethylene 2,5-furandicarboxylate (PEF) based on starch. Abbreviations: 5-(hydroxymethyl)furfural (HMF), 5-(methoxymethyl)furfural (MMF), and 2,5-furandicarboxylic acid (FDCA).



hydrolysis of starch is performed *via* gelatinization, liquefaction, and enzymatic hydrolysis giving rise to highly pure D-glucose syrup, which is in demand in food industry.<sup>39</sup> Hydrolysis of cellulose starts with the pre-treatment of lignocellulosic feedstock to break apart the tightly connected composite of cellulose, hemicelluloses, and lignin. Enzymatic fermentation of the pre-treated lignocellulose results in saccharification of cellulose yielding an aqueous solution of D-glucose. The obtained D-glucose hydrolysate is not as pure as the one prepared based on starch due to the presence of degradation products formed during the pre-treatment. Since these impurities inhibit fermentation of D-glucose, they are removed *via* so-called detoxification procedure. Finally, D-glucose hydrolysate is fermented without an intermediate separation of D-glucose. Cellulosic bioethanol is mainly the target fermentation product at lignocellulosic biorefineries, though production of other value-added compounds is also possible.<sup>40,41</sup>

### 3. Interaction of phenylboronates with saccharides

Boronic acids are remarkable in such a way that they do not donate protons in aqueous solution but rather act as Lewis acids, accepting OH<sup>-</sup> and releasing H<sup>+</sup> (Fig. 4a).<sup>42</sup> Acidity constant of a boronic acid depends on its structure and determines the concentration ratio of a neutral boronic acid to boronate anion at a certain pH value. The neutral and the anionic forms contain trigonal (sp<sup>2</sup>-hybridized) and tetragonal (sp<sup>3</sup>-hybridized) boron, respectively. For the simplest phenylboronic acid, a pK<sub>a</sub> of 8.8 was reported.<sup>43</sup> Boronates are capable of reversible esterification with molecules bearing *vic*-diol moieties as shown in Fig. 4. The complexation constant depends primarily on the stereochemistry of a substrate: polyols and saccharides with *cis*-diol moieties form stronger

complexes than the substrates with *trans*-moieties. The pK<sub>a</sub> value of a boronic acid enables an approximate prediction of an optimum pH value for formation of a boronate-substrate complex. According to the scheme in Fig. 4a, a pH value above the pK<sub>a</sub> value of a boronic acid facilitates its conversion into the boronate anion, which in turn reacts with the substrate to yield the boronate-substrate complex. Nevertheless, several publications report optimal complexation at pH below the pK<sub>a</sub> value of the boronic acid. The reason for this discrepancy is complexation of a substrate with neutral boronic acid moiety to form a boronic acid-substrate complex as depicted in Fig. 4b. Acidity constants of boronic acid-substrate complexes, where the substrate is a saccharide or a polyol, is frequently below the pK<sub>a</sub> value of a parent boronic acid. This results in the formation of a boronate-substrate complex according to the equation in Fig. 4b which takes place at pH values somewhat below the pK<sub>a</sub> values of the boronic acid.<sup>43–46</sup>

Quick and highly specific complexation of boronate with molecules bearing *cis*-diol moieties became the basis of numerous applications. For example, carbohydrate sensors with boronic acid groups were developed.<sup>47–49</sup> Boronic acids have been incorporated in polymeric particles, both as stimuli-responsive functional group and as targeting ligand.<sup>42,48</sup> Boronate affinity chromatography is used to isolate a wide variety of *cis*-diol containing compounds in life science: catechols, nucleosides, nucleotides, nucleic acids, glycoproteins, and enzymes.<sup>48,50–53</sup> Organoboron compounds are used as activating groups for diol motifs found in carbohydrates.<sup>48</sup> Extraction *via* anionic complexation with boronic acids has been explored as means to recover saccharides from the biorefinery streams.<sup>53,54</sup>

Immobilization of boronic acid groups onto cellulose as support to obtain stationary phases for boronate-affinity adsorption was first performed in the 1970s.<sup>55</sup> Since then, various boronate-functionalized materials were prepared and tested for separation of sugar alcohols and saccharides in biorefineries (Table 1).

The adsorbents bearing boronate groups were tested for separation under different modes:

**Simultaneous recovery of few sugars or sugar alcohols from complex solution** presents one example. For instance, D-glucose and D-xylose are simultaneously adsorbed from the hydrolysate of lignocellulose. D-Glucose and D-xylose exist predominantly in pyranose form possessing identical structures.<sup>56</sup> As a result, D-glucose and D-xylose exhibit similar complexation constants with phenylboronate: 65 and 158.<sup>57</sup> Cyclic processes are typically considered for such applications, *i.e.* adsorption at high pH value which favours complexation (Fig. 4 and the description in section 2) followed by desorption taking place under acidic conditions, *i.e.* at pH below pK<sub>a</sub>.

Adsorption of substrates with high and medium complexation constants – for instance, ketoses, aldoses, pentitols, or hexitols – can be readily performed under pH values slightly above pK<sub>a</sub> values of a boronic acid. Desorption of these substrates requires addition of molecular acids or at least CO<sub>2</sub>.<sup>58,59</sup> Adsorption of substrates with low affinity – such as diols or

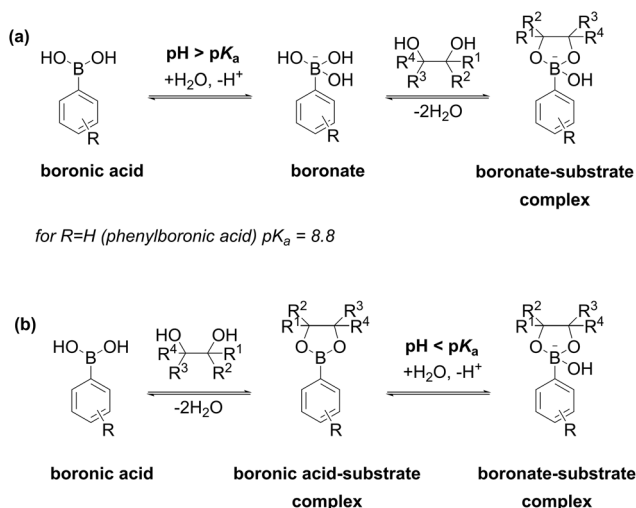


Fig. 4 Two modes of complexation *via* (a) ionization of the boronic acid and (b) its direct complexation with a diol.





**Table 1** Boronate-functionalized adsorbent materials, separation process description, and boron contents

Entry	Process description	Adsorbent	Boron content	Adsorbate loading	Ref.
<b>Gel-type materials</b>					
1	Chromatographic separation of sugars (L-rhamnose, D-mannose, D-galactose, D-glucose, D-ribose, maltose, isomaltose, lactose, and raffinose) using 0.1% aqueous ammonia at pH 10.5 as eluate	“Boric acid gel” 3-Acrylamidophenylboronic acid cross-linked with tetramethylene dimethacrylate	Ca. 1.3 mmol <sub>B</sub> g <sub>polymer</sub> <sup>-1a</sup>	No data	74
2	Chromatographic separation of sugar mixture (D-glucose, D-mannose, D-fructose, D-xylose) with NaOH at pH 9.6 or with pure water	Gel 4-vinylbenzeneboronic acid-divinylbenzene co-polymer	Ca. 4.4 mmol <sub>B</sub> g <sub>polymer</sub> <sup>-1b</sup>	No data	71
3	Recovery of L-erythrose from fermentation broths using frontal chromatography at pH 9.5	Affi-Gel 601 for adsorption	Ca. 0.13 mmol <sub>B</sub> mL <sub>gel</sub> <sup>-1</sup>	6 mg <sub>L-erythrose</sub> mL <sub>gel</sub> <sup>-1</sup>	67
4	Recovery of D-fructose from its mixture with D-glucose; adsorption at pH 10, desorption with CO <sub>2</sub> or acid	Cross-linked 4-vinylphenylboronic acid with 5–40 mol% of a cross-linker	2.9–4.7 mmol <sub>B</sub> g <sub>polymer</sub> <sup>-1</sup>	540 mg <sub>D-fructose</sub> g <sub>polymer</sub> <sup>-1</sup>	58
5	Recovery of diols, polyols, and saccharides; adsorption at high pH, desorption with acid or water	Cross-linked 4-vinylphenylboronic acid with 20 mol% of DVB or EDMA as a cross-linker <sup>c</sup>	3.5–3.7 mmol <sub>B</sub> g <sub>polymer</sub> <sup>-1</sup>	Up to 600 mg g <sub>polymer</sub> <sup>-1</sup>	59
6	Recovery of 2,3-butanediol from fermentation broths	Cross-linked 4-vinylphenylboronic acid with 20 mol% of DVB as a cross-linker <sup>c</sup>	2.6 mmol <sub>B</sub> g <sub>polymer</sub> <sup>-1</sup>	250 mg <sub>2,3-butanediol</sub> g <sub>polymer</sub> <sup>-1</sup>	60
7	Chromatographic separation of D-glucose, D-fructose, and oligosaccharides	Commercial boronate Affi-Gel	1.2–2.5 mmol <sub>B</sub> g <sub>polymer</sub> <sup>-1</sup>	No data	75
<b>Macroporous resins</b>					
8	Recovery of lactulose and D-tagatose; adsorption at pH > 10, desorption at pH 1.5	Poly(3-acrylamidophenylboronic acid-co-ethylene dimethacrylate), 71 or 83 mol% cross-linker	Ca. 1.1–1.45 mmol <sub>B</sub> g <sub>polymer</sub> <sup>-1d</sup>	120–170 mg <sub>lactulose</sub> g <sub>polymer</sub> <sup>-1</sup> , 54 mg <sub>D-tagatose</sub> g <sub>polymer</sub> <sup>-1</sup>	68, 69, 72, 76 and 69
9	Recovery of 1,2,4-butanetriol from fermentation broths; adsorption in NaOH solution, desorption with EtOH or water	Macroporous resin with phenylboronic acid, 2- and 4-naphthalene boronic acid or 4-biphenylboronic acid as functional monomers with 1,3,5-tris(bromomethyl) benzene as a cross-linker, 50 mol% cross-linker	5.5–6.4 mmol <sub>B</sub> g <sub>polymer</sub> <sup>-1e</sup>	Up to 148 mg g <sub>polymer</sub> <sup>-1</sup>	61
<b>Molecularly imprinted polymers</b>					
10	Separation of D-glucose from mixtures with D-xylose; adsorption at pH 11, desorption with 0.5 M HCl	Molecularly imprinted polymer based on methacrylamidophenylboronic acid as functional monomer, methacrylic acid as monomer, ethylene glycol dimethacrylate and methylene-bis-acrylamide as cross-linkers	0.25 mmol <sub>B</sub> g <sub>polymer</sub> <sup>-1f</sup>	Up to 236 mg <sub>D-glucose</sub> g <sub>polymer</sub> <sup>-1</sup>	77
<b>Grafted boronate moieties</b>					
11	Chromatographic separation of sugars (sucrose, D-glucose, D-ribose, and D-fructose) and polyols (erythritol, ribitol, L-arabitol, xylitol, D-mannitol, galactitol, and sorbitol)	Boronate acid groups grafted at cellulosic matrix	0.2–0.6 mmol <sub>B</sub> g <sub>cellulose</sub> <sup>-1</sup>	No data	55 and 78
12	Recovery of lactulose; adsorption at pH 8, desorption at pH 1.5	Grafted boronate groups groups on amino macroporous resin AR-0	2.0 mmol <sub>B</sub> g <sub>polymer</sub> <sup>-1</sup> (AR-1M), 0.66 mmol <sub>B</sub> g <sub>polymer</sub> <sup>-1</sup> (AR-2M)	85 mg <sub>lactulose</sub> g <sub>polymer</sub> <sup>-1</sup>	79
13	Recovery of D-glucose at pH 8.5	Boronic acid functionalized iron oxide	No data	Up to 260 mg <sub>D-glucose</sub> g <sub>material</sub> <sup>-1</sup>	80
14	Recovery of D-fructose from its mixture with D-glucose; adsorption at pH 8, desorption at pH 2	Boronic acid grafted at magnetic nanoparticles	No data	Up to 14.4 mg <sub>D-fructose</sub> g <sub>material</sub> <sup>-1</sup>	81



Table 1 (Contd.)

Entry	Process description	Adsorbent	Boron content	Adsorbate loading	Ref.
15	<i>In situ</i> recovery of D-fructose and D-xylulose during isomerization of D-glucose and D-xylose, respectively	3-Amino phenylboronic acid grafted onto Eupergit C	No data	17 $\mu\text{mol}_{\text{D-fructose}} \text{mL}_{\text{packed bed}}^{-1}$	46
16	Chromatographic separation of D-glucose and D-fructose using sodium pyrophosphate at pH 8.25 as eluate	Silica particles bearing grafted boronate groups	0.25 $\text{mmol}_{\text{B}} \text{g}_{\text{silica}}^{-1}$	No data	82
<b>Grafted polymer brushes</b>					
17	Recovery of D-glucose and D-xylose	Grafted 3-aminophenylboronic acid and grafted brushes with boronate moieties on SBA-15	0.26 $\text{mmol}_{\text{B}} \text{g}_{\text{material}}^{-1}$ (grafted boronate); 1.60 $\text{mmol}_{\text{B}} \text{g}_{\text{material}}^{-1}$ (grafted polymer brushes)	Maximum loadings for grafted boronates: 32 $\text{mg}_{\text{D-xylose}} \text{g}_{\text{material}}^{-1}$ ; 45 $\text{mg}_{\text{D-glucose}} \text{g}_{\text{material}}^{-1}$ ; Maximum loadings for grafted polymer brushes: 372 $\text{mg}_{\text{D-xylose}} \text{g}_{\text{material}}^{-1}$ ; 381 $\text{mg}_{\text{D-glucose}} \text{g}_{\text{material}}^{-1}$ ; 72 $\text{mg}_{\text{D-fructose}} \text{g}_{\text{material}}^{-1}$	56
18	Adsorption of D-fructose in PBS at pH 7.4 <sup>g</sup>	Polymer brushes on silica particles	0.78 $\text{mmol}_{\text{B}} \text{g}_{\text{material}}^{-1}$	72 $\text{mg}_{\text{D-fructose}} \text{g}_{\text{material}}^{-1}$	83
<b>Miscellaneous</b>					
19	Sugars (D-glucose, D-mannose, D-galactose, D-xylose); adsorption at pH 9, desorption by 0.1 M HNO <sub>3</sub>	Cr-based MOF MIL-100 with 5-boronobenzene-1,3-dicarboxylic acid ligand <sup>h</sup>	Up to 0.65 $\text{mmol}_{\text{B}} \text{g}_{\text{material}}^{-1}$	Up to 85 $\text{mg}_{\text{D-galactose}} \text{g}_{\text{material}}^{-1}$	84

<sup>a</sup> Boron content estimated based on data provided in reference.<sup>85</sup> <sup>b</sup> Boron content estimated based on data provided in ref. 71. <sup>c</sup> DVB designates divinylbenzene, EDMA refers to ethylene glycol dimethacrylate. <sup>d</sup> Boron content estimated based on data provided in reference.<sup>76</sup> <sup>e</sup> Estimated by the authors based on energy-dispersive X-Ray spectroscopy (EDS) analysis in reference.<sup>61</sup> <sup>f</sup> Estimated based on the composition of the polymer provided by the authors of reference.<sup>77</sup> <sup>g</sup> PBS designates phosphate-buffered saline. <sup>h</sup> MOF refers to metal-organic framework, MIL refers to Materials of Institute Lavoisier.

triols – require addition of more equivalents of NaOH. However, these weakly bonded substrates can be readily desorbed by washing with water, ethanol, or water-ethanol mixtures.<sup>59–61</sup>

**Isolation of a target product from a mixture of similar molecules** has been the goal of numerous studies. Most frequently, the separation is based on differences of complexation constants of the adsorbates.<sup>59</sup> Separation of an aldose and a corresponding 2-ketose presents a classic example of substrates suitable for separation by adsorption on boronate-bearing materials. Isomerization of D-glucose into D-fructose is of great interest as a method for production of HFCS (Fig. 5a). Isomerization of D-glucose into D-fructose results in *ca.* 42% product yield in a commercial process performed at 60 °C owing to thermodynamic and kinetic limitations; consequently, the obtained reaction mixture requires separation.<sup>36</sup> D-Glucose is an aldose which takes up pyranose forms in aqueous solution. Aldopyranoses in general and D-glucose in particular do not exhibit any *cis*-diol moieties, which leads to weak complexation of aldopyranoses with boronate moieties. Complexation of ketoses is typically significantly stronger than of aldoses (*cf.* complexation constants of 65 and 1698 for D-glucose and D-fructose, respectively, since  $\beta$ -D-fructofuranose and  $\beta$ -D-fructopyranose conformers exhibit *cis*-diol moieties, Fig. 5b).<sup>59</sup> The presence of *cis*-diol groups enables a selective adsorption of D-fructose, whereas D-glucose remains in solution.<sup>58</sup> Exploration of molecular boronate complexes suggested

formation of 2,3-fructofuranose and 1,2-fructopyranose complexes (Fig. 5c).<sup>62</sup> In addition to 1:1 complexes between D-fructose and the boronate moiety, MAS NMR of the adsorbed D-fructose species suggested complexation of saccharide and boronate moiety with 1:2 stoichiometry.<sup>58</sup>

**Ketoses** of commercial interest which can be selectively recovered from the corresponding reaction mixtures are shown in Fig. 6. The aldodisaccharide lactose is readily available as by-product from dairy industry. Isomerization of lactose (Fig. 6a) into the corresponding ketodisaccharide lactulose has received considerable attention in recent years due to its increasing commercial value in the pharmaceutical, nutraceutical, and food industries. Lactulose has been registered in over 100 countries as a medicinal drug and is on the World Health Organization Model List of Essential Medicines, a database of the most important medications required in a basic health system.<sup>63,64</sup> D-Galactose (Fig. 6b) presents an aldohexose readily available as a monomer of hemicellulosic polysaccharides<sup>26</sup> or a disaccharide lactose.<sup>65</sup> Isomerization of D-galactose gives rise to a rare sugar D-tagatose with sweetness similar to that of sucrose. Importantly, D-tagatose presents a low-caloric sweetener, exhibits a low glycemic index, and shows prebiotic effect. Isomerization of D-xylose results in D-xylulose, which is in demand for synthesis of fine chemicals and can be considered as intermediates for synthesis of bio-based bulk chemicals such as furfural (Fig. 6c).<sup>11,66</sup> L-Erythrulose is a rare C4 ketose which can be produced *via* the *Escherichia coli* trans-



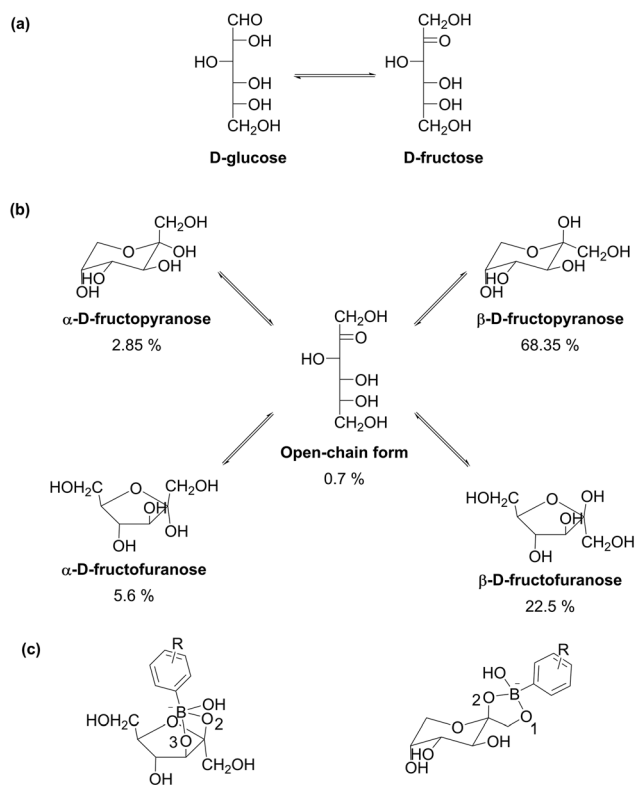


**Fig. 5** (a) Isomerization of D-glucose into D-fructose; (b) equilibrium forms of  $[2-^{13}\text{C}]\text{-D-fructose}$  determined by  $^{13}\text{C}$  NMR at 25 °C in  $\text{D}_2\text{O}$  as solvent;<sup>70</sup> (c) complexes between boronate anions and anomers of D-fructose.<sup>62</sup>

ketolase-catalyzed condensation of glycolaldehyde and  $\beta$ -hydroxy pyruvate (Fig. 6d).<sup>67</sup>

The separation of ketoses is often performed in a cyclic batch adsorption mode: at elevated pH values in the range of 7.5–12, ketoses are adsorbed, whereas the rest of the components, *i.e.* the remaining substrates, catalysts, and eventually auxiliaries, remain in the liquid phase. Desorption of the

ketoses under acidic conditions is possible. Frequently, small portions of aldose are co-adsorbed with ketose. Thus, desorption of such a binary mixture can be performed in two steps to improve their purity. Wang *et al.* explored desorption of less strongly adsorbed D-galactose and more strongly adsorbed D-tagatose. The first step of desorption presents treatment of the loaded resin with distilled water at pH *ca.* 6; under these conditions, D-galactose (complexation constant with phenylboronate 126)<sup>57</sup> is readily desorbed, whereas D-tagatose (complexation constant with phenylboronate 1995)<sup>57</sup> remains mostly adsorbed. The second step of desorption is treatment with an acid at pH below 2, leading to desorption of D-tagatose of high purity.<sup>68</sup> The same approach was applied to produce high-purity lactulose.<sup>69</sup>

Selective adsorptive uptake of ketoses offers an opportunity for process intensification *via* development of adsorption-assisted synthetic methods. *In situ* product removal facilitates an equilibrium shift towards the product and mitigates the product inhibition of biocatalyzed processes. Materials bearing boronate moieties can be added directly into a reactor: improvement of yield of D-fructose from below 30% to 50.1% upon isomerization catalyzed by NaOH at pH 12 was reported.<sup>71</sup> Similarly, a 56% yield of D-fructose was obtained by performing isomerization-adsorption cycles.<sup>58</sup> *In situ* and recycling experiments enabled adsorption-assisted processes with high yields of lactulose of up to 72%<sup>69,72</sup> and of D-tagatose of 53%.<sup>68</sup> A circulating set-up containing a reactor operating at elevated temperature and an adsorption column at room temperature enabled 56.7% yield of D-fructose.<sup>71</sup> Adsorption onto boronate-bearing materials was used for *in situ* product isolation for isomerization of D-glucose into D-fructose and D-xylose into D-xylulose catalyzed by glucose isomerase. *In situ* adsorption improved the yields of D-fructose from 45% to 73% and of D-xylulose from 23% to 52%.<sup>46</sup> L-Erythrulose was adsorbed by *in situ* product removal during the *Escherichia coli* transketolase-catalyzed condensation of glycolaldehyde and lithium  $\beta$ -hydroxy pyruvate resulting in improved productivity of the bioconversion.<sup>67</sup>

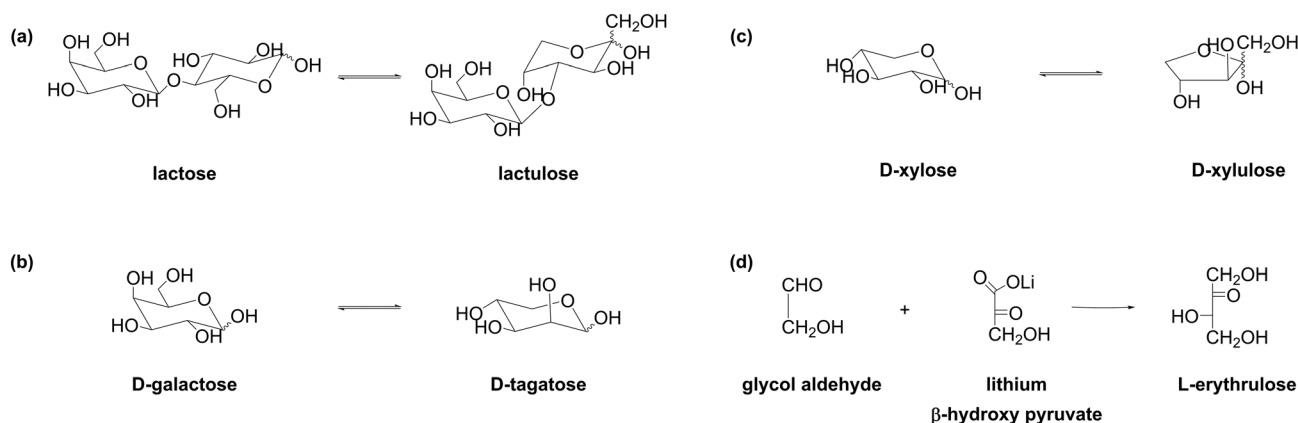


**Fig. 6** (a) Isomerization of D-lactose into D-lactulose; (b) isomerization of D-galactose into D-tagatose; (c) isomerization of D-xylose into D-xylulose; (d) conversion of glycolaldehyde and  $\beta$ -hydroxy pyruvate into L-erythrulose in the presence of *Escherichia coli* transketolase.



Importantly, not only affinity of a particular substrate towards boronate moieties but also other factors, for instance, a porous structure of an adsorbate, can be employed to control the selectivity of uptake. The concept of molecular imprinting implies creation of an artificial keyhole which exhibits an exact match to geometrical dimensions of the target molecule.<sup>73</sup> A selective recovery of D-glucose from its mixture with D-fructose and D-xylose *via* selective adsorption on a molecularly imprinted polymer functionalized with phenylboronate moieties has been recently reported. Section 4.3 provides more details on synthesis and structural peculiarities of molecularly imprinted polymers.

Chromatographic separation over materials functionalized with boronate groups as stationary phases was investigated.<sup>74</sup> A potential separation and recovery of all components of the complex mixture is a significant advantage of chromatographic separation compared to the adsorption method described above. In general, chromatographic separation remains the most frequently used separation technique for recovery of sugar alcohols and sugars in industry.<sup>25</sup> Dilution of the recovered product with an eluate, which should be removed by evaporation, presents the major drawback of chromatography. A few authors reported a correlation between the substrate structure and its tendency to complexation. An increase in the number of *cis*-hydroxyl groups results in more extensive complex formation and, consequently, larger retention times at the stationary phases bearing boronate groups.<sup>55,71,74</sup>

## 4. Adsorbent

Table 1 summarizes different boronate-functionalized adsorbent materials and the corresponding separation procedures. The adsorbent types are discussed in detail in this section.

### 4.1. Gel-type polymers

Gel-type polymers (Table 1, entries 1–7) can be readily prepared *via* radical polymerization of 4-vinylphenylboronic acid with addition of a small amount of a cross-linker. Commercial availability of 4-vinylphenylboronic acid as well as of the cross-linkers presents an advantage of this method (Fig. 7). Moreover, gel-type polymers contain high amount of boron and exhibit therefore high maximal adsorption capacity: the boron content of up to  $4.7 \text{ mmol}_{\text{boron}} \text{ g}_{\text{polymer}}^{-1}$  was reported.<sup>58</sup> Alternatively, boron-containing Affi-Gel with as high boron content as  $1.2\text{--}2.5 \text{ mmol}_{\text{boron}} \text{ g}_{\text{polymer}}^{-1}$  in dry state is commercially available from Bio rad.<sup>75</sup> Though these gels are produced *via* immobilization of boronate moieties, they exhibit a gel-type matrix and will be considered in this section.

Adsorption affinity of diols, polyols, and saccharides can be readily predicted based on their well-documented molecular complexation constants with phenylboronic acid.<sup>57</sup> In line with this, elution order of the saccharides on the column was reported to be dependent on the complexation ability.

Gel-type polymers are nonporous in dry state and can swell in different solvents. Schroer *et al.* synthesized gel-type poly-

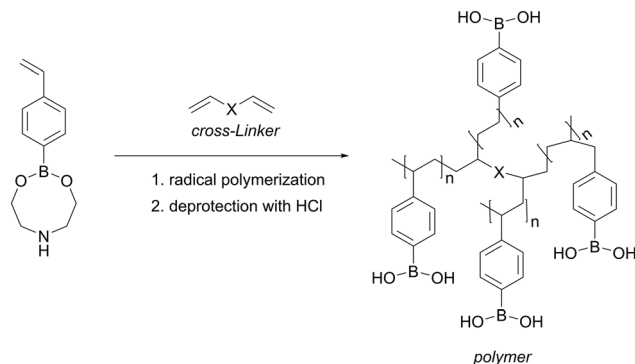


**Fig. 7** Synthesis of a cross-linked gel-type polymer. This figure has been adapted from ref. 58 with permission from the Royal Society of Chemistry, copyright 2020.

mers with various types of linkers (Fig. 8a) and examined adsorption of D-fructose and D-glucose on the adsorbed polymers. D-Fructose presents an adsorbate with high affinity towards complexation (complexation constant is 1698).<sup>57</sup> It is readily adsorbed on the outer shell of the polymer particle, and the polymer chains get negatively charged. Repulsion of the negatively charged polymer chains results in further swelling, making the boronate groups in the polymer core accessible, and further adsorption of D-fructose occurs. Maximum capacity of the polymer depends on the structure of the cross-linker: long aliphatic or stiff aromatic cross-linkers were favourable for an efficient transport of D-fructose towards the boronate sites (Fig. 8b). Thus, equimolar uptakes of D-fructose were possible for the materials bearing these cross-linkers, *i.e.*

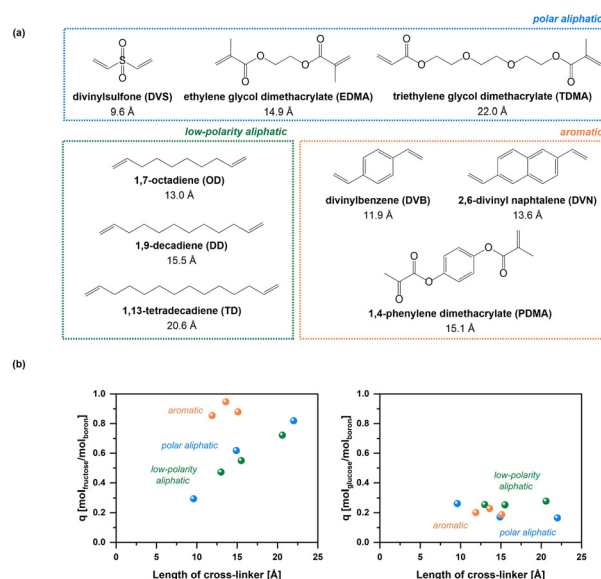


**Fig. 8** (a) Structures of the cross-linkers used to synthesize gel-type polymers with boronate moieties and (b) dependency of loadings of D-fructose (left) and D-glucose (right) on the nature of the cross-linker. This figure has been adapted from ref. 58 with permission from the Royal Society of Chemistry, copyright 2020.







**Fig. 9** Scheme of swelling upon adsorption of D-fructose and D-glucose. This figure has been adapted from ref. 58 with permission from the Royal Society of Chemistry, copyright 2020.

1 mol D-fructose for 1 mol boron (Fig. 9). It is noteworthy that the capacity depends on the amount of a cross-linker: an increase of DVB content from 5 mol% to 40 mol% resulted in a decrease of a maximum uptake of D-fructose of  $1 \text{ mol}_{\text{D-fructose}} \text{ mol}_{\text{boron}}^{-1}$  to  $0.5 \text{ mol}_{\text{D-fructose}} \text{ mol}_{\text{boron}}^{-1}$ .<sup>56</sup> This result is expected since the pore size of gel-type microporous polymers is determined by the percentage of the used cross-linking monomer.<sup>86</sup> Smaller pore size leads to lower uptake owing to worse accessibility of the boronate sites.

D-Glucose exhibits a significantly lower affinity to polymers functionalized with boronate moieties, which corroborates with its lower molecular complexation constant with phenylboronic acid of 65.<sup>57</sup> Consequently, D-glucose is adsorbed on the outer shell of polymer in lower amount, leading to a lower charge of the polymer chains and, consequently, a lower swelling degree. As a result, most of the boronate sites remain inaccessible for D-glucose (Fig. 9).<sup>58</sup>

Schroer *et al.* investigated adsorption of 18 diols, sugar alcohols, and saccharides on gel-type poly(4-vinylphenylboronic acid) cross-linked with 20 mol% DVB or 20 mol% EDMA. The authors concluded that the adsorption mechanism schematically shown on Fig. 9 can be generalized: the adsorbates with high complexing constants readily induce swelling of the polymers and exhibit loadings of 1 mol substrate per 1 mol boronate group which corresponds to maximum loadings of up to  $600 \text{ mg}_{\text{substrate}} \text{ g}_{\text{polymer}}^{-1}$  in carbonate buffer at pH 10, estimated using Langmuir adsorption model. Very high loadings were observed for instance, for D-sorbitol (complexation constant 10232), D-xylitol (complexation constant 2399), D-mannitol (complexation constant 2089), or D-tagatose (complexation constant 1995).<sup>59</sup>

The adsorbates with low complexation constants adsorb on the outer shell of the polymer particle and low density of the negative charge on the polymer chains does not cause a significant swelling. An example of such adsorbates is glycerol with a complexation constant of 16, which exhibits a moderate

loading of *ca.*  $80 \text{ mg}_{\text{glycerol}} \text{ g}_{\text{polymer}}^{-1}$  in carbonate buffer at pH 10. It is nevertheless possible to reach high loadings of adsorbates with low affinity by adding more equivalents of a base. As Fig. 4a suggests, increase of  $\text{OH}^-$  concentration results in a shift of the equilibrium to the right. For 2,3-butanediol, the complexation constant is 3.5. In carbonate buffer at pH 10, only  $160 \text{ mg}_{2,3\text{-butanediol}} \text{ g}_{\text{polymer}}^{-1}$  was obtained. However, the capacity could be increased to  $250 \text{ mg}_{2,3\text{-butanediol}} \text{ g}_{\text{polymer}}^{-1}$  corresponding to an equimolar loading with respect to boron content upon addition of at least 1 equivalent of NaOH to one equivalent of substrate.<sup>60</sup>

Cyclic adsorption operations with boronate materials typically imply adsorption under basic and desorption under acidic conditions. However, placing the swollen loaded gel-type polymers into an acidic or neutral solution causes shrinkage of the materials.<sup>87</sup> As a result, the adsorbate molecules located at the core of the polymer bead experience significant diffusional hindrances which leads to “trapping” of part of the desorbed adsorbate in the core of the shrunk resin and hinders a full recovery.<sup>58,59</sup>

A narrow peak shape and a good separation factor at high loading of the adsorbate are important factors for preparative chromatography. Barker *et al.* explored elution of D-glucose and D-fructose on a gel-type column using NaOH solution at pH 9.6 as a mobile phase. For low-concentration samples, sugars were eluted as symmetrical peaks, but the peak of D-fructose was broad with respect to D-glucose and D-mannose. Increase of a sugar loading from 250  $\mu\text{g}$  to 500 mg resulted in a significant decrease of the retention factor of D-fructose and a peak tailing. The authors explained this effect by a considerable local increase in acidity due to complex formation at high concentration of D-fructose (Fig. 4b).<sup>71</sup> At the same time, neutralization owing to injection of highly-concentrated D-fructose, which also exhibits acidic properties, cannot be excluded. Very high swelling degrees of the functionalized with boronates loaded gel-type polymers are well documented.



Vente *et al.* observed volume increase of an adsorbent swollen in NaOH by a factor of 2.57 for commercial Boronate Affi-Gel.<sup>75</sup> Schroer *et al.* reported 212% swelling degree in the presence of D-fructose in carbonate buffer at pH 10 for a gel-type 4-vinylphenylboronic acid polymer cross-linked with 20 mol% DVB.<sup>58</sup> Such high swelling degrees suggest high elasticities and poor mechanical strength hampering large scale applications. Moreover, Vente *et al.* conducted column separation using gel-type Boronate Affi-Gel as a stationary phase, which was pre-swollen by washing with a NaOH solution at pH 9. Injection of D-fructose resulted in a decrease of pH to 6, a partial conversion of boronate groups into boronic acid groups (Fig. 4), and a shrinkage of the chromatographic bed.<sup>75</sup>

Though gel-type polymers with an optimized structure and an appropriate content of cross-linker are capable of high loadings of adsorbates with high complexation affinities, the rates of the adsorption are low. Thus, it takes typically 5–7 h to reach saturation loading of D-fructose on the poly(4-vinylphenylboronic acid) cross-linked with 20 mol% DVB at room temperature. The unfavourable kinetics may be explained by the time required for the polymer to swell as well as a slow substrate diffusion in the micropore structure of the swollen gel.<sup>58,59</sup>

Gel-type polymers bearing phenylboronic acid moieties are hydrophobic and not wettable by aqueous solutions of the adsorbates. Batch adsorption experiments required addition of an organic solvent, *e.g.* ethanol, as a co-solvent to improve wettability.<sup>58,59</sup> Vente *et al.* performed column experiments and reported on improvement of hydrophilicity upon transformation of boronic acid groups into boronate groups.<sup>75</sup>

#### 4.2. Macroporous resins

Macroporous resins are prepared with higher contents of cross-linkers than gel-type polymers (Table 1, entries 8 and 9). Macroporous (also referred to as macroreticular or isoporous) polymer particles constitute of an agglomerate made of secondary particles representing agglomerates of microspheres themselves.<sup>73</sup>

The adsorption sites located inside of these microspheres become unavailable due to a high degree of cross-linking<sup>88</sup> resulting in lower capacities of macroporous resins compared to gel-type materials. Transport of adsorbates into meso- and macropores between the agglomerates is quicker than into the microporous gel. Moreover, higher mechanic stability of macroporous resins than of highly elastic microporous gels is an advantage for their large-scale application.

The groups of Hua and Yang synthesized macroporous resins by radical polymerization using 3-acrylamidophenylboronic acid as a functional monomer, ethylene dimethacrylate as a cross-linker, and DMSO as a porogen (Fig. 10).<sup>76</sup> A series of adsorbents varying the content of a cross-linker in the range of 50 to 93 mol% was prepared. The authors reported that the two materials containing 71 and 83% of the cross-linker, respectively, exhibited the best performance in terms of lactulose loading. Boron content was in the range of *ca.* 1.1 to 1.45 mmol<sub>boron</sub> g<sub>polymer</sub><sup>-1</sup>, whereas the maximal loading of lac-



**Fig. 10** A method to produce a macroporous resin bearing boronic acid groups developed by Wang *et al.* This figure has been reproduced from ref. 76 with permission from the Elsevier, copyright 2019. Abbreviations: 3-acrylamidophenylboronic acid (AAPBA), ethylene glycol dimethylacrylate (EGMA), and dimethylsulfoxide (DMSO).

tulose was 120–170 mmol<sub>lactulose</sub> g<sub>polymer</sub><sup>-1</sup>. This suggests that 30–50% of the total boronate groups are complexed at maximum loading of lactulose. Very quick adsorption of lactulose required less than 15 minutes at pH 10 and an almost instant ( $\leq 5$  min) desorption at pH below 2 was reported. The prepared macroporous materials were used for *in situ* recovery of lactulose from the mixture obtained after isomerization of lactose catalyzed by Na<sub>2</sub>HPO<sub>4</sub> + NaOH as well as for separation of D-tagatose from a reaction mixture after isomerization of D-galactose with NaOH at pH 12.<sup>68,69,72,76</sup>

Meng *et al.* explored Friedl–Crafts alkylation reaction to prepare macroporous resins functionalized with boronate moieties. The authors used phenylboronic acid, 1-naphthaleneboronic acid, 4-biphenylboronic acid, or 2-naphthaleneboronic acid as functional monomers and 1,3,5-methylboronate benzene as a cross-linker (Fig. 11).

A functional monomer and a cross-linker were taken in equimolar amounts and polymerized in DCM using AlCl<sub>3</sub> as a catalyst. The resin prepared based on 2-naphthaleneboronic acid exhibited the highest saturated adsorption capacity of

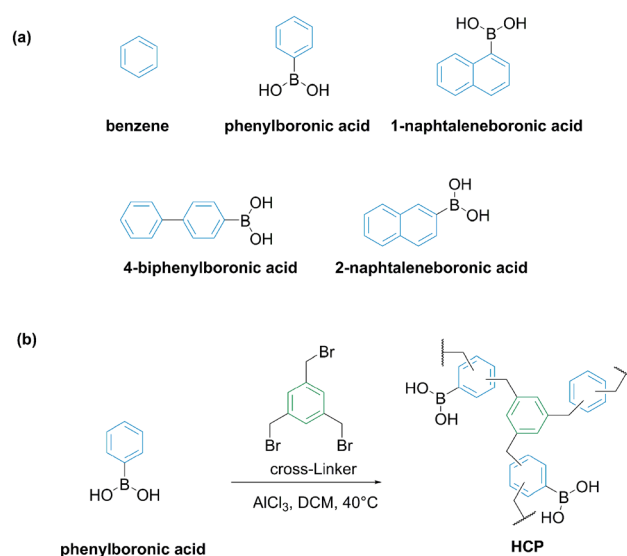


**Fig. 11** (a) Functional monomers for the manufacture of the polymers; (b) Friedel–Crafts method to synthesize boronate containing macroporous resins.<sup>61</sup>



1,2,4-butanetriol of  $148.2 \text{ mg g}_{\text{polymer}}^{-1}$ . The authors estimated the boron content based on Energy-dispersive X-ray spectroscopy (EDS) analysis as 6–7%. Thus, for the resin based on 2-naphthaleneboronic acid, the highest loading of 1,2,4-butanetriol corresponded to 0.25 mol adsorbate per mol boron. The materials exhibited permanent porosity and specific surface area of  $800\text{--}1200 \text{ m}^2 \text{ g}^{-1}$ . A quick establishment of an equilibrium in a time shorter than 10 minutes was reported. 1,2,4-Butanetriol could be recovered by desorption with water or ethanol.<sup>61</sup>

### 4.3. Molecular imprinting

The concept of molecular imprinting was introduced by Mosbach and Wulff in the 1970s.<sup>73</sup> Molecularly imprinted materials are prepared *via* cross-linking of a functional monomer complexed with a target adsorbate. Washing out the adsorbate enables formation of a cavity of certain geometry resulting in a shape selectivity for adsorption. Keeping the geometrical parameters of the artificial keyhole constant under adsorption and desorption conditions requires a high rigidity of the polymer matrix, which can be reached by a very high content of a cross-linker. Nevertheless, application of molecularly imprinted polymers found limited application in preparative chromatography owing to a few disadvantages. High content of a cross-linker results in a low content of a functional monomer and, consequently, in low adsorption capacities. Typical adsorption capacities of molecularly imprinted materials are in the range of  $0.5\text{--}10 \text{ mg}_{\text{D-fructose}} \text{ g}_{\text{polymer}}^{-1}$ .<sup>89,90</sup> Moreover, a highly cross-linked matrix of the

polymer leads to serious diffusion limitations resulting in significant peak tailing.<sup>73</sup>

Interestingly, Liu *et al.* recently reported a polymer design based on the monomers shown in Fig. 12 (Table 1, entry 10). The authors used D-glucose (1 mmol) as a template, methacrylamidophenylboronic acid (MAAPBA, 1.2 mmol) as a functional monomer, methacrylic acid (MAA, 6.8 mmol) as a monomer, ethylene glycol dimethacrylate (EGDMA, 19 mmol) as a hydrophobic cross-linker, and methylene-bis-acrylamide (MBAA, 1 mmol) as a hydrophilic cross-linker. The ratio of hydrophilic-to-hydrophobic cross-linkers was found to influence the adsorbate uptake. The material was molecularly imprinted with D-glucose, and a higher adsorption selectivity for D-glucose than for D-xylose despite similar complexation constants (complexation constants for D-glucose and D-xylose are 65 and 158, respectively) was reported.<sup>59</sup> Rates of adsorption were low as the adsorption required 4 hours. A remarkable uptake of D-glucose of  $236 \text{ mg}_{\text{D-glucose}} \text{ g}_{\text{polymer}}^{-1}$  for adsorption at pH 11 was reported, being significantly higher than typically observed for molecularly imprinted polymers. Interestingly, estimation of boron content based on the ratio of monomers provided by the authors ( $0.25 \text{ mmol}_{\text{boron}} \text{ g}_{\text{polymer}}^{-1}$ ) suggests the theoretical capacity of D-glucose of *ca.*  $46 \text{ mg}_{\text{D-glucose}} \text{ g}_{\text{polymer}}^{-1}$ . Moreover, unexpectedly high loadings of D-glucose on the molecularly imprinted polymer of  $76\text{--}79 \text{ mg}_{\text{D-glucose}} \text{ g}_{\text{polymer}}^{-1}$  at acidic pH values of 3–5 were reported. Understanding the reasons of the observed high capacities under different adsorption conditions remains of great interest. Liu *et al.* tested a hollow-fiber membrane system containing the synthesized molecularly imprinted polymer aiming at

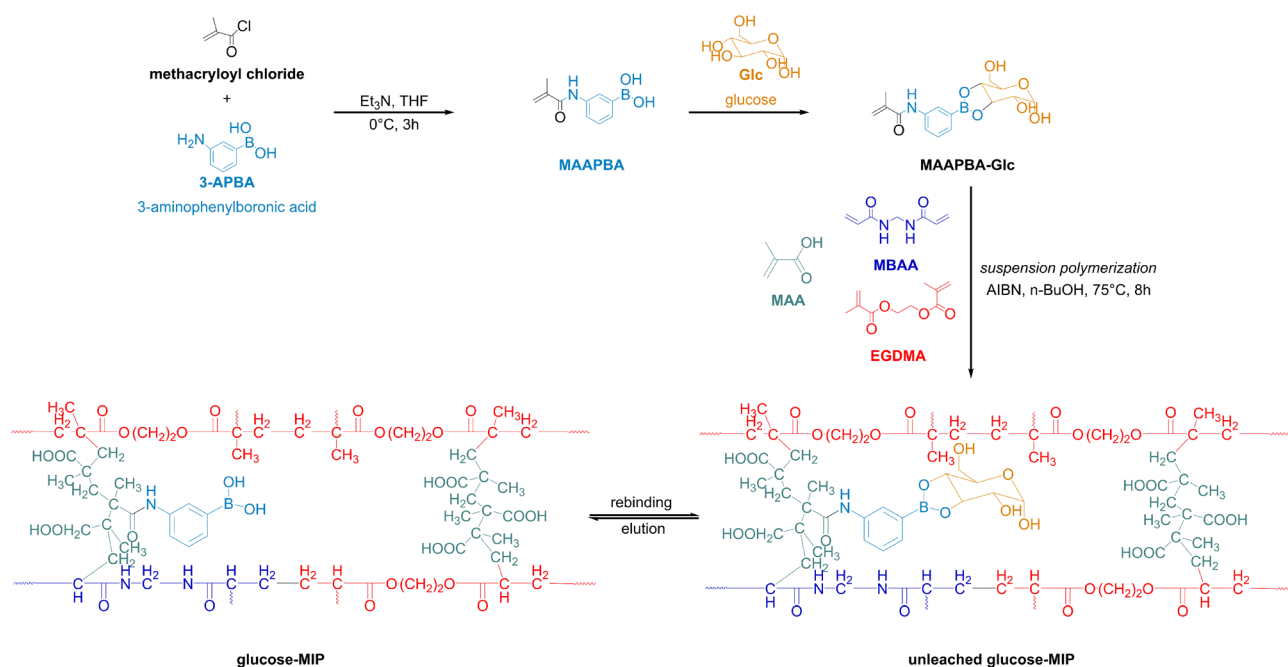


**Fig. 12** Molecularly imprinted polymer for a selective capture of D-glucose from cellulose hydrolysates. This figure has been reproduced from ref. 77 with permission from the John Wiley and Sons, copyright 2022. Abbreviations: 3-acrylamidophenylboronic acid (AAPBA), methacrylic acid (MAA), *N,N'*-methylenebisacrylamide (MBAA), ethylene glycol dimethylacrylate (EGMA), azobisisobutyronitrile (AIBN).



a selective capture of D-glucose from cellulose hydrolysates. A higher adsorption capacity of D-glucose under static than under dynamic conditions was reported which was explained by slow kinetics of adsorption.<sup>77</sup>

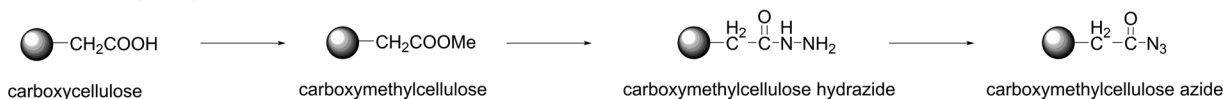
#### 4.4. Grafted boronate moieties

Historically, phenylboronate groups grafted on an inert core (Table 1, entries 11–16) constructed the first boronate-containing stationary phase fabricated by Weith *et al.* in 1970 for separation of saccharides, polyols, nucleosides, and deoxynucleosides.<sup>55</sup> The authors chose cellulose as an insoluble matrix to avoid diffusion limitations and proposed two multistep methods for grafting dihydroxyboryl groups shown in Fig. 13. First, commercially available carboxymethylcellulose was converted in its hydrazide and then to azide. Treatment of the obtained material with *m*-aminobenzeneboronic acid resulted in formation *N*-(*m*-dihydroxyborylphenyl)-carbamiylmethylcellulose containing 0.2 mmol boronic acid groups per gram of dry cellulose (Route 1, Fig. 13). To obtain the second material, *m*-aminobenzeneboronic acid was converted into *N*-(*m*-dihydroxyborylphenyl)succinamic acid by reaction with succinic anhydride, and the condensation of this acid in aqueous solution with aminoethylcellulose in the presence of *N*-cyclohexyl-*N'*-β-(4-methylmorpholinium)ethylcarbodiimide *p*-toluenesulfonate as the activation agent to yield *N*-[*N'*-(*m*-dihydroxyborylphenyl)succinamyl]aminoethylcellulose bearing 0.6 mmol boronic acid groups per gram of dry cellulose (Route 2, Fig. 13). Interestingly, the material prepared based on carboxymethylcellulose (Route 1, Fig. 13) contained some amount of the negatively charged COO<sup>−</sup> groups. On the contrary, utilization of aminoethylcellulose as a starting material

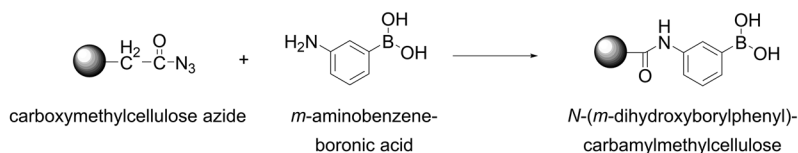
gave rise to the stationary phase contained some amount of positively charged NH<sub>3</sub><sup>+</sup> groups (Route 2, Fig. 13). The authors performed column separation of saccharides, polyols, nucleosides, and deoxynucleosides on a column filled with the synthesized stationary phases using solutions at constant pH values of 7.5 or 8.5. The results suggested that the grafted negatively charged COO<sup>−</sup> caused an increase of p*K*<sub>a</sub> of the grafted dihydroxyboryl groups, whereas the grafted positively charged NH<sub>3</sub><sup>+</sup> groups led to decrease of the p*K*<sub>a</sub> values of boronic acid moieties. Interestingly, increase of the ionic strength of an eluate led to diminishing of these effects.<sup>55</sup>

Wang *et al.* recently prepared two materials *via* grafting boronic acid groups on a macroporous NH<sub>2</sub>-containing resin AR-0 with a content of −NH<sub>2</sub> functional groups of *ca.* 6.4 mmol<sub>NH<sub>2</sub></sub> g<sub>dry resins</sub><sup>−1</sup>. The synthetic methods and the boron contents reported by the authors are shown in Fig. 14. The resin was pre-swollen in DMF prior to grafting of the boronate functionalities. The resin AR-1M was obtained by covalent bonding of *p*-formylphenylboronic acid to the surface of AR-0 producing the Schiff's base which was reduced by addition of sodium cyanohydride powder in methanol. In the second route, glutaraldehyde was first grafted to AR-0 resin followed by addition of 3-aminophenylboronic acid yielding the Schiff's base. The latter was reduced by addition of sodium cyanohydride powder in methanol resulting in the resin AR-2M. The boron contents of AR-1M and AR-2M were 2.0 and 0.66 mmol<sub>boron</sub> g<sub>polymer</sub><sup>−1</sup>, respectively. The resins were tested for adsorption of lactulose, the maximum substrate loading was reported for the AR-1M material amounting to 85 mg g<sub>resin</sub><sup>−1</sup>. This corresponds to 0.12 equivalents of the adsorbate to 1 equivalent of boron. For AR-2M polymer, a higher complexation

#### Synthesis of carboxymethylcellulose azide



#### Route 1



#### Route 2

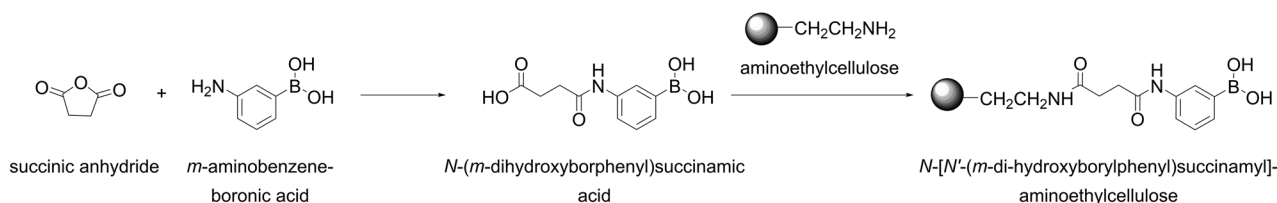


**Fig. 13** Two different routes for the grafting of boronic acid onto cellulose proposed by Weith *et al.* This figure has been reproduced from ref. 55 with permission from the American Chemical Society, copyright 1970.





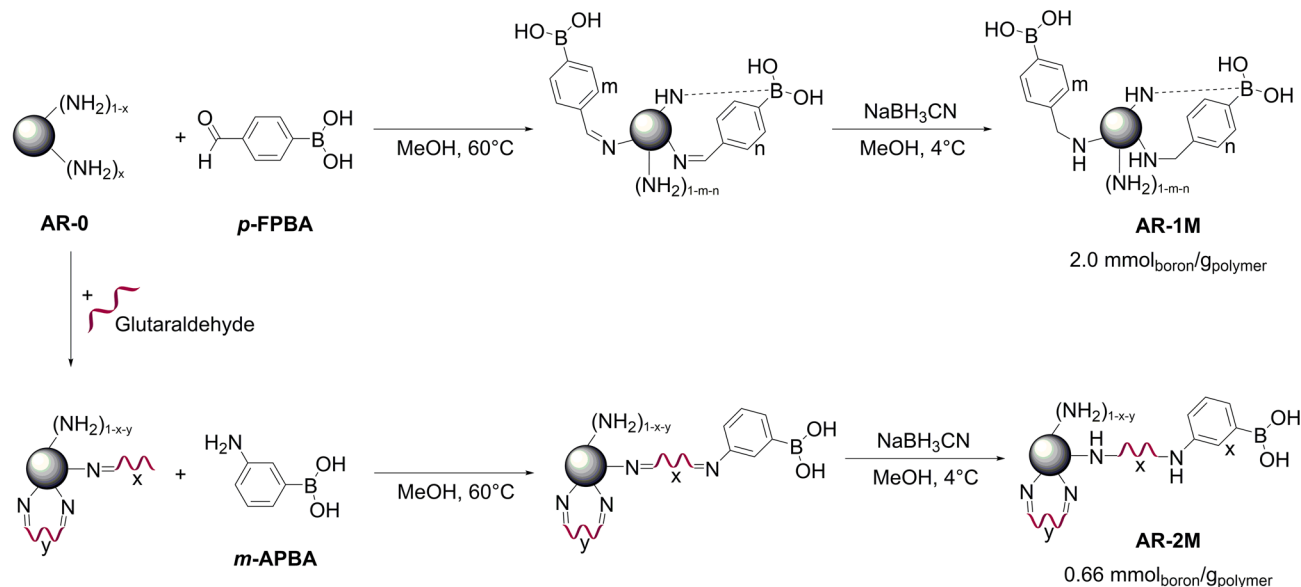


**Fig. 14** Synthetic routes for grafting phenylboronic acid moieties onto an amino microporous resin proposed by Wang *et al.* This figure has been reproduced from ref. 79 with permission from the American Chemical Society, copyright 2018. Abbreviations: aminated macroporous poly(styrene-co-divinylbenzene) resin (AR-0), *p*-formylphenylboronic acid (*p*-FPBA), 3-aminophenylboronic acid (*m*-APBA).

degree of 22% could be attained. The reasons of rather low loadings of lactulose per boron equivalent were not discussed by the authors and can probably be explained by swelling of the AR-0 resin in DMF prior to the grafting. Probably, shrinking in aqueous phase led to low accessibility of the grafted adsorption sites. Slow kinetics of adsorption and acid-induced desorption requiring 3–4 h and 1–2 h, respectively, support the hypothesis of not readily accessible boronate groups. Adsorption under basic conditions resulted in a selective adsorption of lactulose with separation factors of 2–16. Dependency of lactulose uptake by AR-1M and AR-2M resins on pH value is remarkable: the highest lactulose capacity were observed at pH values of 6 and 8 for the materials synthesized *via* grafting of aldehyde and amine, respectively. Further increase of the pH value till 10 did not result in improvement of the uptake. The authors explained this effect by the presence of residual surface  $\text{-NH}_2$  groups responsible for alkaline microenvironment and capable of forming B–N-coordination complexes similar to these in Wulff type phenylboronic acids (Fig. 14).<sup>79</sup>

Functionalization of  $\text{Fe}_3\text{O}_4$  to prepare magnetically separable nanoparticles bearing boronate groups was conducted according to the scheme shown in Fig. 15. 3-Aminophenylboronic acid was allowed to react with 3,4-dihydroxybenzaldehyde; the obtained derivative was grafted onto  $\text{Fe}_3\text{O}_4$  nanoparticles to yield functionalized particles of the size of  $8 \pm 2$  nm. The boron content was not reported, but the synthesized nanoparticles exhibited a high uptake of D-glucose of up to  $260 \text{ mg}_{\text{D-glucose}} \text{ g}_{\text{material}}^{-1}$  in phosphate buffer at pH 8.5. Unfortunately, the authors did not report the results of desorption, which would be of interest since desorption at low pH values could result in leaching of iron.<sup>80</sup>

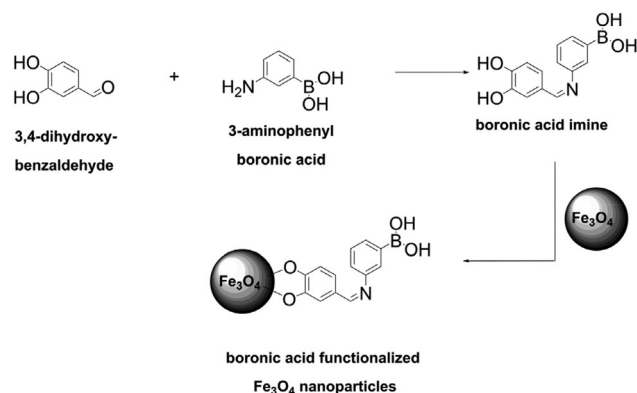


**Fig. 15** Functionalization of  $\text{Fe}_3\text{O}_4$  nanoparticles with boronic acid moieties performed by Mohapatra *et al.* This figure has been reproduced from ref. 80 with permission from the Elsevier, copyright 2009.

Gu *et al.* also prepared functionalized  $\text{Fe}_3\text{O}_4$  magnetic nanoparticles. For these purpose,  $\text{Fe}_3\text{O}_4$  nanoparticles were first coated with  $\text{SiO}_2$  using sol-gel reaction, thereafter a thiol-containing moiety was immobilized followed by grafting of 4-vinylphenylboronic acid *via* a thiol-ene click reaction. The nanoparticles had a mean diameter of 195 nm. Unfortunately, the authors did not provide information on boron content. The functionalized nanoparticles exhibited a moderate maximal adsorption capacity of D-fructose of *ca.*  $14.4 \text{ mg}_{\text{D-fructose}} \text{ g}_{\text{material}}^{-1}$  at pH 8.0. D-Glucose could be desorbed at pH 2 and the nanoparticles could be reused 6 times.<sup>81</sup> Immobilization of 3-aminophenylboronic acid on a commercial Eupergit Gel also resulted in a binding capacity of D-fructose corresponding to  $17 \mu\text{mol mL}^{-1}$  bed or  $3.06 \text{ mg mL}^{-1}$  bed at pH 8.0.<sup>46</sup> Glad



*et al.* proposed a method to load 3-aminophenylboronic acid on small 10  $\mu\text{m}$  silica particles according to the scheme shown in Fig. 16.

First, silica was modified with  $\gamma$ -glycidopropyltrimethoxysilane; 3-aminobenzene boronic acid was grafted onto the modified surface. The authors fabricated small particles for HPLC rather than large particles applied for low-pressure chromatography (typically, the particles size of stationary phases applied in low-pressure chromatography is in the range of 50 to 200  $\mu\text{m}$ )<sup>91</sup> aiming at reduction of diffusion contri-

butions. HPLC enables higher flow rates of an eluate associated with larger pressure drops. The obtained material contained 0.250 mmol boron per gram. The authors reported a baseline HPLC separation of D-glucose and D-fructose as peaks without tails with a buffer solution at pH 8.3 used as eluate.<sup>82</sup>

In summary, grafting of boronate groups results in highly accessible adsorption sites on tailored support. Low content of boron and, consequently, low capacity of an adsorbent present the major disadvantages of this preparative method.

**4.4.1. Grafted polymer brushes.** Grafted polymer brushes (Table 1, entries 17 and 18) are similar to grafted boronate sites though the former exhibit increased boron loadings. Zhao *et al.* demonstrated this advantage for the first time by a comparative study of grafted 3-aminophenyl boronic acid and grafted polymer brushes with a boronate functionality. The authors used SBA-15 as support and performed the syntheses as Fig. 17 shows. In the first route, a coupling agent was used to link a boronic acid and SBA-15, whereas in the second route poly(acrylic acid) brushes were generated at the surface of SBA-15 by surface-initiated atom transfer radical polymerization (ATRP) and 3-aminophenylboronic acid was then immobilized. Remarkably, the materials bearing grafted boronates and polymer brushes exhibited 0.26  $\text{mmol}_{\text{boron}} \text{g}_{\text{material}}^{-1}$  and 1.60  $\text{mmol}_{\text{boron}} \text{g}_{\text{material}}^{-1}$  boron content, respectively. In accordance with this, the maximum uptake of D-glucose esti-

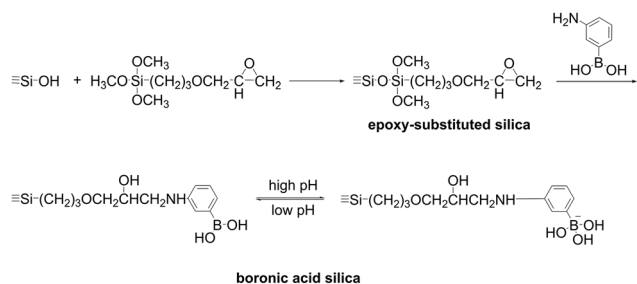


**Fig. 16** Grafting of boronate moieties onto silica support. This figure has been reproduced from ref. 82 with permission from the Elsevier, copyright 1980.

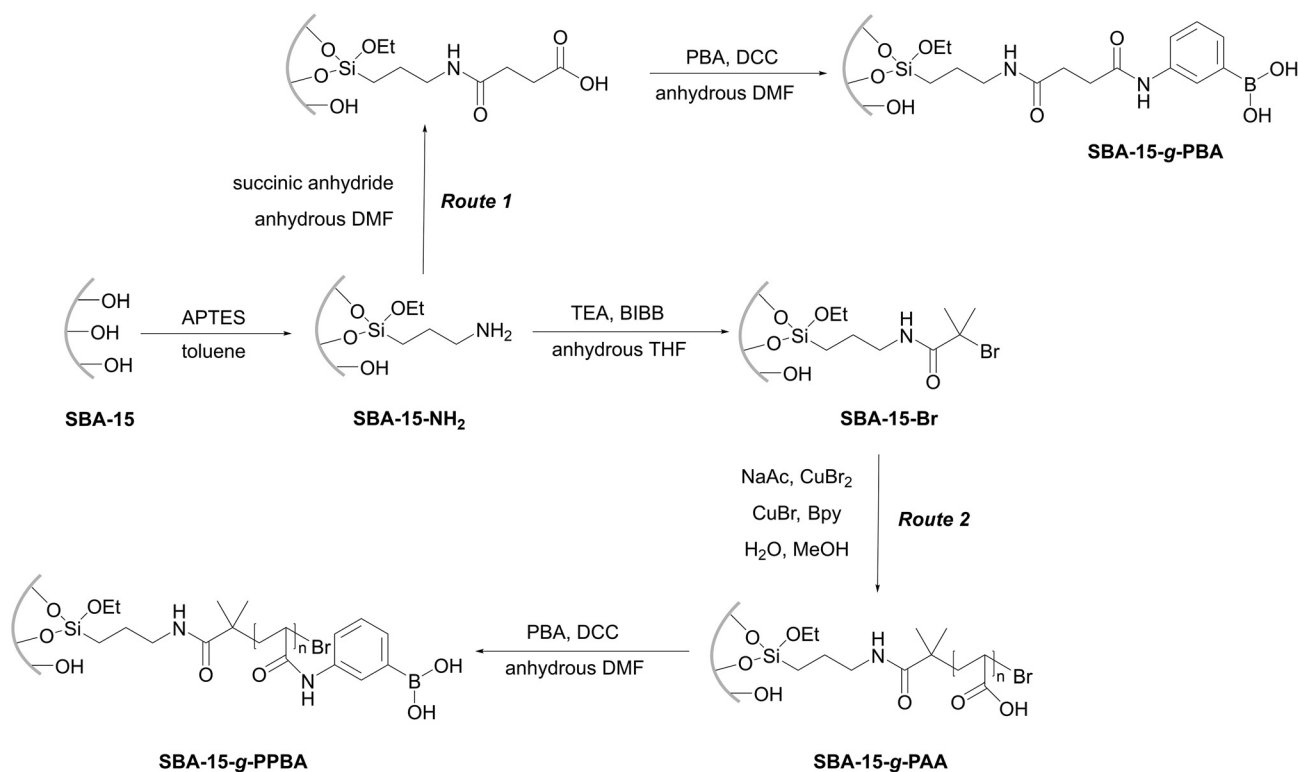


**Fig. 17** Grafting 3-aminophenyl boronic acid (Route 1) or polymer brushes (Route 2) with boronate moieties onto SBA-15 proposed by Zhao *et al.* This figure has been reproduced from ref. 56 with permission from the American Chemical Society, copyright 2011. Abbreviations: 3-aminophenylboronic acid (PBA), *N,N'*-dicyclohexylcarbodiimide (DCC), *N,N*-dimethylformamide (DMF), mesoporous silica Santa Barbara Amorphous-15 (SBA-15), (3-aminopropyl)triethoxysilane (APTES), triethylamine (TEA), 2-bromoisobutyryl bromide (BIBB), tetrahydrofuran (THF), and 2,2'-bipyridyl (bpy).



mated in the scopes of a Langmuir model for the material with grafted boronate and for the material with polymer brushes were  $45 \text{ mg}_{\text{D-glucose}} \text{ g}_{\text{material}}^{-1}$  and  $381 \text{ mg}_{\text{D-glucose}} \text{ g}_{\text{material}}^{-1}$ , respectively. An improved uptake of D-xylose on the material with functionalized grafted polymer brushes was also reported (Table 1, entry 17). Zhao *et al.* explored adsorption of D-glucose and D-xylose in the batch experiments from the solutions at pH of 8.7 adjusted with NaOH. The measured uptake of the sugars suggested a 1:1 stoichiometry of adsorbate-to-boron supporting the hypothesis of an improved accessibility of boron grafted as polymer brushes. Interestingly, the adsorption was not quick, and *ca.* 3–4 hours were required until the equilibrium was reached. It can be explained by location of the polymer brushes in pores of SBA-15, leading to drop of specific surface area of SBA-15 from  $940 \text{ m}^2 \text{ g}^{-1}$  for the unfunctionalized material to *ca.*  $0 \text{ m}^2 \text{ g}^{-1}$  for the material with grafted polymer brushes. Apparently, pore blockage hampers diffusion into the pores of SBA-15 filled with the grafted polymers.<sup>56</sup>

Xu *et al.* also prepared polymer brushes on the silica particles using ATRP. The authors aimed at preparation of a fluorescent grafted polymer brush bearing boronic acid polymer. For this purpose, a fluorescent boronic acid monomer was first prepared from an azide-tagged boronic acid and an alkyne-containing acrylate using a CuAAC click chemistry reaction. Next, the boronic acid monomer was grafted on the surface of silica gel modified with an ATRP initiator (Fig. 18). The authors reported boron loading of  $0.78 \text{ mmol}_{\text{boron}} \text{ g}_{\text{material}}^{-1}$  and observed  $72 \text{ mg g}^{-1}$  loading of D-fructose in phosphate buffered saline (PBS) at pH 7.4.<sup>83</sup>

**4.4.2. Miscellaneous.** In 2015, Zhu *et al.* reported the first example of metal organic frameworks by integrating Cr-based MOFs of MIL with boronic acid containing ligands (Table 1, entry 19). Boron content of up to  $0.6 \text{ mmol}_{\text{boron}} \text{ g}_{\text{MOF}}^{-1}$  was reported. The authors applied the material for adsorption of a mixture of D-glucose, D-mannose, D-xylose, and D-galactose at pH 9 reaching the highest loading of D-galactose of  $95 \text{ mg}$

$\text{g}_{\text{MOF}}^{-1}$ . This indicates that 85% of boronate moieties participate in complexation. Desorption was performed by washing with  $0.1 \text{ M HNO}_3$  and the material was successfully recycled 5 times.<sup>84</sup>

## 5. Performance of boronate-functionalized materials vs. $\text{Ca}^{2+}$ ion-exchanged resins: state of the art and outlook

Materials bearing boronate moieties are not the only stationary phases capable of adsorptive separation of sugar alcohols and saccharides. Chromatographic separation of saccharides using other adsorbates, such as materials functionalized with amino groups,<sup>92–94</sup> ion-exchange resin in  $\text{HCO}_3^-$  form,<sup>95</sup> or anion-exchange resin in bisulfite form,<sup>93,96</sup> is well known. Nevertheless, these types of stationary phases – as well as the materials with boronate moieties – are not used for large-scale preparative processes. The reasons for limited application of these separation methods to laboratory scale are organic co-eluates required for separation on amine stationary phases<sup>93</sup> or low stability of bisulfites against oxidation by molecular oxygen leading to conversion of bisulfite groups into sulfate groups.<sup>75</sup> Development of material science opens further opportunities for synthesis of stationary phases. For instance, separation of D-glucose and D-fructose by pore exclusion of zirconium-based metal-organic frameworks was recently reported.<sup>97</sup>

Gel-type slightly cross-linked cation exchange resins in  $\text{Ca}^{2+}$  form are most frequently used for recovery of sugars and polyols,<sup>98,99</sup> for instance, for separation of D-fructose and D-glucose after the isomerization (Fig. 5a) as one of the largest separation processes of biomass-based compounds. Separation of saccharides over  $\text{Ca}^{2+}$ -containing materials was occasionally uncovered by Felicetta *et al.* in 1959: separating the sugars from spent sulfite liquors from the lignin sulfonates using ion-exchange resins, the authors observed separation of L-arabinose and D-xylose.<sup>99</sup> In the 1970s,  $\text{Ca}^{2+}$  exchanged resins were explored and industrialized as stationary phases for large-scale chromatographic separation of D-fructose and D-glucose. Ligand exchange presents the main mechanism responsible for the separation. In aqueous solution, hydroxyl groups of saccharides compete with the coordinated water molecules at  $\text{Ca}^{2+}$  ion. Single  $\text{OH}^-$  groups of carbohydrates cannot compete with the solvent, only a suitably arranged combination of two (axial-equatorial) or three (axial-equatorial-axial) hydroxyl groups results in a significant complex formation with  $\text{Ca}^{2+}$ .<sup>100</sup> The isomers bear the following numbers of the axial-equatorial pairs of  $\text{OH}^-$ -groups: glucopyranose (1/0 for  $\alpha/\beta$ ), fructopyranose (1/2 for  $\alpha/\beta$ ), and fructofuranose (1/0 for  $\alpha/\beta$ ).<sup>98</sup> Consequently, stronger complexation of D-fructose than of D-glucose results in a larger retention volume of the former. Tiihonen *et al.* explored complexation of the saccharides with  $\text{Ca}^{2+}$  and concluded on a weak complexation of D-fructose with

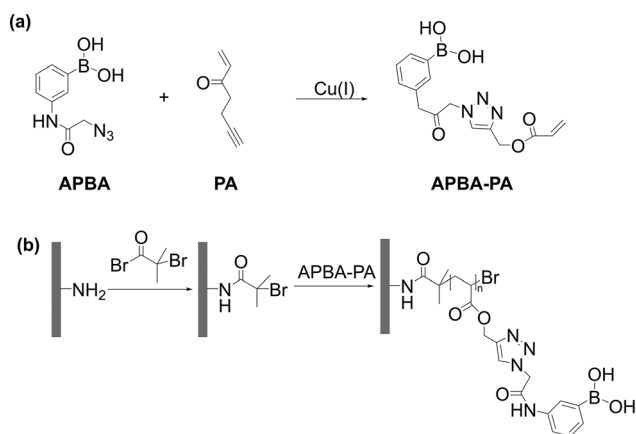


**Fig. 18** (a) Synthesis of boronic acid monomer and (b) its polymerization using surface-initiated ATRP. Reproduced with permission from ref. 83. Abbreviations: 3-(2-azido-acetylamino)phenylboronic acid (APBA) and propargyl acrylate (PA).



$\text{Ca}^{2+}$  and a very weak complexation of D-glucose with  $\text{Ca}^{2+}$ .<sup>101</sup> This result corroborates with other publications, which suggest partition into gel matrix of the ion-exchange resin as the main mechanism responsible for retention of D-glucose, implying that D-glucose is not really adsorbed in a formal sense but merely occupies the intraparticle pore space in direct proportion to its concentration in the fluid.<sup>102</sup>

Application of pure water as eluate presents a remarkable advantage of the separation over the  $\text{Ca}^{2+}$  ion exchange resins. It implies a low-cost and an environmentally benign eluate which requires no desalination. Warm water, typically of 55–60 °C, is used: increase of temperature is necessary to reduce pressure drop when operating at high concentrations of the sugars.<sup>102</sup> Further advantages of  $\text{Ca}^{2+}$  ion exchange resins are low cost and commercial availability of the stationary phase, high long-term stability of the phase without regeneration, and a high column capacity.<sup>99</sup> Moreover, the equilibrium isotherms of D-glucose and D-fructose are linear up to high concentrations of ca. 260 g L<sup>-1</sup>.<sup>103</sup> This is of utmost importance for preparative chromatography since high concentrations and high loadings are typical of preparative mode. Linear adsorption isotherms are prerequisite for symmetric peaks without tailing.<sup>104</sup> Noteworthy, moderate separation factors of D-glucose and D-fructose in the range of 2.5–3.5 present a disadvantage of  $\text{Ca}^{2+}$  ion exchange resins.<sup>105,106</sup>

Traditional batch chromatography implies injection of a solution to be separated followed by elution. Batch chromatography is usually characterized by high dilution of the obtained fractions which requires an energy-intensive evaporation of eluate. In order to reduce the consumption of eluate, an advanced simulated moving bed (SMB) mode is used on an industrial scale for separation of D-glucose and D-fructose. SMB presents a continuous countercurrent fluid-solid separation developed by UOP under the name of “Sorbex” in the 1970s.<sup>105,107</sup>

The first reports on materials bearing boronate groups as stationary phases for separation of sugar alcohols and saccharides were published at the same time as the publications on separations using  $\text{Ca}^{2+}$  ion exchange resins. However, adsorbents functionalized with boronates have not been commercialized yet. A necessity to use buffer solutions rather than pure water presents a crucial point limiting applicability of boronate-containing stationary phases. This challenge was addressed by Barker *et al.* who examined a boronate gel as a stationary phase and water as eluate and reported sharp peaks for non-adsorbed sugars, such as D-glucose and D-mannose, tailed peaks for D-fructose and D-xylose, and a very broad peak for D-ribose. The tailing was explained by acidification of the solution due to complexation of sugars with dihydroxyboron groups (Fig. 4b).<sup>71</sup> Interaction of a specific boronic acid with *cis*-diol groups is highly dependent on pH and  $\text{pK}_a$  of the boronic acid. In most of the applied materials, phenylboronate or naphthalene boronate were used as adsorption sites (Table 1), *i.e.* the acids with  $\text{pK}_a$  of ca. 9. Consequently, the pH value of ca. 9 for a suitable ionization degree is expected, whereas in pure water a pH value of ca. 6 is observed.

Moreover, ionization of a complex of a substrate with a boronic acid moiety (Fig. 4b) can be responsible for local pH drop. Barker *et al.* suggested application of boronic acids with lower  $\text{pK}_a$  values as functional monomers in order to keep a significant part of the boronate ionized at pH close to 6.7. Ionization constants of boronic acids depend on their structures, and phenylboronic acids with low  $\text{pK}_a$  values are commercially available.<sup>52</sup> A lack of functionality enabling polymerization of these commercial phenylboronic acids presents a major challenge. Fortunately, rapid development of x-omics, particularly proteomics, metabolomics, and glycomics in recent years, resulted in an increased interest to boronate affinity materials. Consequently, syntheses of novel functional monomers, a few examples of which are shown in Fig. 19 and whose synthetic routes were recently reviewed,<sup>52</sup> were proposed. Barker *et al.* suggested that a half-neutralized solution of a boronic acid will act as a buffer and thus it is possible for a resin to be self-buffering if the eluent pH is equal to the  $\text{pK}_a$  value for the acid.<sup>71</sup> In addition to application of monomers with lower  $\text{pK}_a$  values, modification of the materials with amine functionalities holds promise to decrease the pH of adsorption.<sup>79</sup>

Furthermore, optimization of the porous structure of the adsorbents bearing phenylboronic acid groups to enable a quick access to all the boron adsorption sites are required (Table 1). Gel-type polymers exhibit high swelling degrees of up to 250% and are therefore of limited mechanical strength; macroporous resins do not enable access to all the adsorption sites; and supported boronate groups exhibit low boron loadings resulting in low capacities. Polymer brushes of polymerized functional monomers appear to be promising adsorbent offering high boron loading along with accessibility of the adsorption centers. However, this type of materials remains underexplored. Shaping and pelletizing of the adsorbent beads has been rarely addressed in the literature.<sup>69,79,82</sup> At the same time, shape and size distribution of the adsorbent particles used in a fixed bed is of great importance for hydrodynamics and diffusion contribution and, consequently, for efficiency of the separation.

Process design based on adsorption over materials bearing boronate groups presents another crucial milestone to develop convincing and competitive separation processes for biorefineries. Current research activity is mainly focused on cyclic

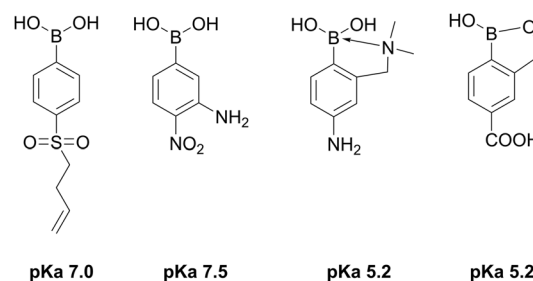


Fig. 19 Examples of boronate monomers exhibiting low  $\text{pK}_a$  values.<sup>108–111</sup>





adsorption–desorption processes with adsorption under basic and desorption under acidic conditions. Advances enabling a continuous separation process, such as SMB chromatography or cyclic batch adsorption process, and minimizing desalting of the eluates are necessary for further development. Aqueous solutions of saccharides and sugar alcohols are commercially used nowadays in food, cosmetic, or pharmaceutical industries. Production of saccharides and sugar alcohols as intermediates in novel value chains will probably require other solvents for fractionation demanding a re-design of production and separation processes. Conversion of D-fructose into a mixture of HMF and MMF using methanol with a few per cents of water as a solvent in Avantium process (Fig. 2) presents one example of saccharide transformation in an organic solution.

## 6. Conclusion

Saccharides and sugar alcohols are expected to play important roles in novel value chains based on biomass raw materials. Separation of these compounds from complex and frequently diluted product streams poses a challenge which can be tackled *via* selective adsorption of saccharides and sugar alcohols on tailored materials. Chromatographic separations on Ca<sup>2+</sup> ion exchange resins are the state-of-the-art recovery techniques which sometimes suffer from low separation efficiency of the components over these stationary phases. Development of novel materials exhibiting higher separation factors provides opportunities for design of more efficient separation methods. In this regard, material bearing phenylboronic acid moieties are of utmost interest owing to high affinity of the boronate sites towards saccharides and polyols. An ideal adsorbent should exhibit a large boron content along with high accessibility of the adsorption sites, high mechanical stability owing to low tendency to swell, and a tailored porous structure enabling quick diffusion rates. Molecular structure of an adsorption site determines the pK<sub>a</sub> values of the boronic acid moieties. Synthesis of materials with low pK<sub>a</sub> values of the boronic acid sites are of utmost interest since these adsorbents are potentially capable of adsorption in pure water. Engineering processes of the adsorptive separation without a need for desalination of an eluate presents another crucial task to be solved for development of economically beneficial and environmentally benign separations. Overall, great versatility of materials bearing boronate moieties opens numerous opportunities for development of advanced separation processes.

## Author contributions

Irina Delidovich: conceptualisation, formal analysis, writing – original draft, funding acquisition. Valérie Toussaint: conceptualisation, writing – review & editing.

## Conflicts of interest

There are no conflicts to declare.

## Acknowledgements

We gratefully acknowledge financial support of the German Research Foundation (Deutsche Forschungsgemeinschaft, DFG Project 450360023).

## References

- 1 A. Duwe, N. Tippkötter and R. Ulber, in *Biorefineries*, ed. K. Wagemann and N. Tippkötter, Springer International Publishing, Cham, 2019, pp. 177–215.
- 2 N. Dahmen, E. Henrich and T. Henrich, in *Biorefineries*, ed. K. Wagemann and N. Tippkötter, Springer International Publishing, Cham, 2019, pp. 217–245.
- 3 A. Jess and P. Wasserscheid, *Chemical Technology: an Integrated Textbook*, Wiley, 2013.
- 4 T. Werpy and G. R. Petersen, *Top value added chemicals from biomass Volume I- Results of screening for potential candidates from sugars and synthesis gas*, Washington, DC, 2004.
- 5 J. J. Bozell and G. R. Petersen, *Green Chem.*, 2010, **12**, 539–554.
- 6 G. W. Huber, S. Iborra and A. Corma, *Chem. Rev.*, 2006, **106**, 4044.
- 7 J. N. Chheda, G. W. Huber and J. A. Dumesic, *Angew. Chem., Int. Ed.*, 2007, **46**, 7164.
- 8 R. Rinaldi and F. Schuth, *Energy Environ. Sci.*, 2009, **2**, 610–626.
- 9 P. Gallezot, *Chem. Soc. Rev.*, 2012, **41**, 1538–1558.
- 10 M. Yabushita, H. Kobayashi and A. Fukuoka, *Appl. Catal., B*, 2014, **145**, 1–9.
- 11 I. Delidovich, P. J. C. Hausoul, L. Deng, R. Pfützenreuter, M. Rose and R. Palkovits, *Chem. Rev.*, 2016, **116**, 1540–1599.
- 12 J. Artz and R. Palkovits, *Curr. Opin. Green Sustainable Chem.*, 2018, **14**, 14–18.
- 13 L. T. Mika, E. Cséfalvay and Á. Németh, *Chem. Rev.*, 2018, **118**, 505–613.
- 14 A. Jaswal, P. P. Singh and T. Mondal, *Green Chem.*, 2022, **24**, 510–551.
- 15 L. Goswami, R. Kayalvizhi, P. K. Dikshit, K. C. Sherpa, S. Roy, A. Kushwaha, B. S. Kim, R. Banerjee, S. Jacob and R. C. Rajak, *Chem. Eng. J.*, 2022, **448**, 137677.
- 16 I. Delidovich, K. Leonhard and R. Palkovits, *Energy Environ. Sci.*, 2014, **7**, 2803–2830.
- 17 S. Venkatesan, in *Sep. Purif. Technol. Biorefineries*, 2013, pp. 101–148.
- 18 G. P. van Walsum, in *Sep. Purif. Technol. Biorefineries*, 2013, pp. 513–532.



- 19 S.-T. Yang and C. Lu, in *Sep. Purif. Technol. Biorefineries*, 2013, pp. 409–437.
- 20 Z. Lei and B. Chen, in *Sep. Purif. Technol. Biorefineries*, 2013, pp. 37–60.
- 21 J. Zhang and B. Hu, in *Sep. Purif. Technol. Biorefineries*, 2013, pp. 61–78.
- 22 M. Ayoub and A. Z. Abdullah, *Renewable Sustainable Energy Rev.*, 2012, **16**, 2671–2686.
- 23 A. A. Babadi, S. Rahmati, R. Fakhlaei, B. Barati, S. Wang, W. Doherty and K. Ostrikov, *Biomass Bioenergy*, 2022, **163**, 106521.
- 24 H. Schiweck, A. Bär, R. Vogel, E. Schwarz, M. Kunz, C. Dusautois, A. Clement, C. Lefranc, B. Lüssem, M. Moser and S. Peters, in *Ullmann's Encyclopedia of Industrial Chemistry*, 2012.
- 25 E4tech, RE-CORD and WUR, "From the Sugar Platform to biofuels and biochemicals". Final report for the European Commission, Contract No. ENER/C2/423-2012/SI2.673791, 2015.
- 26 L. Negahdar, I. Delidovich and R. Palkovits, *Appl. Catal., B*, 2016, **184**, 285–298.
- 27 B. G. Harvey, W. W. Merriman and R. L. Quintana, *ChemSusChem*, 2016, **9**, 1814–1819.
- 28 P. Drabo, T. Tiso, B. Heyman, E. Sarikaya, P. Gaspar, J. Förster, J. Büchs, L. M. Blank and I. Delidovich, *ChemSusChem*, 2017, **10**, 3252–3259.
- 29 J.-P. Lange, *ChemSusChem*, 2017, **10**, 245–252.
- 30 R.-J. van Putten, J. C. van der Waal, E. de Jong and H. J. Heeres, *Carbohydr. Res.*, 2017, **446**, 1–6.
- 31 B. F. M. Kuster, *Starch – Stärke*, 1990, **42**, 314–321.
- 32 H. E. van Dam, A. P. G. Kieboom and H. van Bekkum, *Starch – Stärke*, 1986, **38**, 95–101.
- 33 R.-J. van Putten, J. C. van der Waal, M. Harmse, H. H. van de Bovenkamp, E. de Jong and H. J. Heeres, *ChemSusChem*, 2016, **9**, 1827–1834.
- 34 E. De Jong, H. Stichnothe, G. Bell and H. Jorgensen, *Biobased chemicals: a 2020 update*, 2020.
- 35 S. Wu, R. Snajdrova, J. C. Moore, K. Baldenius and U. T. Bornscheuer, *Angew. Chem., Int. Ed.*, 2021, **60**, 88–119.
- 36 L. M. Hanover and J. S. White, *Am. J. Clin. Nutr.*, 1993, **58**, 724S–732S.
- 37 J.-P. Lange, E. van der Heide, J. van Buijtenen and R. Price, *ChemSusChem*, 2012, **5**, 150–166.
- 38 K. Siroth and K. Piyachomkwan, *Bioprocessing Technologies in Biorefinery for Sustainable Production of Fuels, Chemicals, and Polymers*, 2013, pp. 27–46.
- 39 A. Läufer, *Biorefineries*, 2019, 137–152.
- 40 V. Menon and M. Rao, *Prog. Energy Combust. Sci.*, 2012, **38**, 522–550.
- 41 A. K. Chandel, V. K. Garlapati, A. K. Singh, F. A. F. Antunes and S. S. da Silva, *Bioresour. Technol.*, 2018, **264**, 370–381.
- 42 A. Stubelius, S. Lee and A. Almutairi, *Acc. Chem. Res.*, 2019, **52**, 3108–3119.
- 43 G. Springsteen and B. Wang, *Tetrahedron*, 2002, **58**, 5291–5300.
- 44 J. Yan, G. Springsteen, S. Deeter and B. Wang, *Tetrahedron*, 2004, **60**, 11205–11209.
- 45 R. P. Singhal, B. Ramamurthy, N. Govindraj and Y. Sarwar, *J. Chromatogr. A*, 1991, **543**, 17–38.
- 46 A. Dukler and A. Freeman, *Biotechnol. Bioeng.*, 2001, **75**, 25–28.
- 47 S. D. Bull, M. G. Davidson, J. M. H. van den Elsen, J. S. Fossey, A. T. A. Jenkins, Y.-B. Jiang, Y. Kubo, F. Marken, K. Sakurai, J. Zhao and T. D. James, *Acc. Chem. Res.*, 2013, **46**, 312–326.
- 48 C. A. McClary and M. S. Taylor, *Carbohydr. Res.*, 2013, **381**, 112–122.
- 49 T. D. James, K. R. A. S. Sandanayake and S. Shinkai, *Angew. Chem., Int. Ed. Engl.*, 1996, **35**, 1910–1922.
- 50 X.-C. Liu and W. H. Scouten, in *Affinity Chromatography: Methods and Protocols*, ed. P. Bailon, G. K. Ehrlich, W.-J. Fung and W. Berthold, Humana Press, Totowa, NJ, 2000, pp. 119–128.
- 51 M. B. Espina-Benitez, J. Randon, C. Demesmay and V. Dugas, *Sep. Purif. Rev.*, 2018, **47**, 214–228.
- 52 D. Li, Y. Chen and Z. Liu, *Chem. Soc. Rev.*, 2015, **44**, 8097–8123.
- 53 P. J. Duggan, *Aust. J. Chem.*, 2004, **57**, 291–299.
- 54 H. C. Ferraz, L. T. Duarte, M. Di Luccio, T. L. M. Alves, A. C. Habert and C. P. Borges, *Braz. J. Chem. Eng.*, 2007, **24**, 101–118.
- 55 H. L. Weith, J. L. Wiebers and P. T. Gilham, *Biochemistry*, 1970, **9**, 4396–4401.
- 56 Y.-H. Zhao and D. F. Shantz, *Langmuir*, 2011, **27**, 14554–14562.
- 57 J. A. Peters, *Coord. Chem. Rev.*, 2014, **268**, 1–22.
- 58 G. Schroer, J. Deischer, T. Zensen, J. Kraus, A.-C. Pöppler, L. Qi, S. Scott and I. Delidovich, *Green Chem.*, 2020, **22**, 550–562.
- 59 G. Schroer, V. Toussaint, S. Bachmann, A.-C. Pöppler, C. H. Gierlich and I. Delidovich, *ChemSusChem*, 2021, **14**, 5207–5215.
- 60 G. Schroer, V. Toussaint, B. Heyman, J. Büchs, A.-C. Pöppler and I. Delidovich, *Curr. Res. Green Sustainable Chem.*, 2022, **5**, 100297.
- 61 Q. Meng, M. Rong, H. Xing, J. Yu, Y. Wang, X. Wei, R.-A. Chi, C. Chen, H. Liu and L. Yang, *Sep. Purif. Technol.*, 2023, **314**, 123436.
- 62 I. Delidovich and R. Palkovits, *Green Chem.*, 2016, **18**, 5822–5830.
- 63 M. Wang, L. Wang, X. Lyu, X. Hua, J. M. Goddard and R. Yang, *Biotechnol. Adv.*, 2022, **60**, 108021.
- 64 P. Khuwijitjaru, N. Milasing and S. Adachi, *Sci. Eng. Health Stud.*, 2018, **12**, 159–167.
- 65 S. Cheng, L. E. Metzger and S. I. Martínez-Monteaudo, *Sci. Rep.*, 2020, **10**, 2730.
- 66 V. Choudhary, A. B. Pinar, S. I. Sandler, D. G. Vlachos and R. F. Lobo, *ACS Catal.*, 2011, **1**, 1724–1728.
- 67 R. P. Chauhan, L. W. Powell and J. M. Woodley, *J. Appl. Biotechnol. Bioeng.*, 1997, **56**, 345–351.



- 68 Z. Wang, M. Wang, X. Lyu, C. Wang, Y. Tong, X. Hua and R. Yang, *Chem. Eng. J.*, 2022, **446**, 137089.
- 69 M. Wang, L. Wang, X. Hua and R. Yang, *Food Chem.*, 2023, **429**, 136935.
- 70 P. Drabo, M. Fischer, M. Emondts, J. Hamm, M. Engelke, M. Simonis, L. Qi, S. L. Scott, R. Palkovits and I. Delidovich, *J. Catal.*, 2023, **418**, 13–21.
- 71 S. A. Barker, B. W. Hatt, P. J. Somers and R. R. Woodbury, *Carbohydr. Res.*, 1973, **26**, 55–64.
- 72 X. Zhu, M. Wang, X. Hua, C. Yao and R. Yang, *Chem. Eng. J.*, 2021, **406**, 126751.
- 73 M. Schulte, in *Preparative Chromatography*, 2020, pp. 49–157.
- 74 K. Reske and H. Schott, *Angew. Chem., Int. Ed. Engl.*, 1973, **12**, 417–418.
- 75 J. A. Vente, H. Bosch, A. B. de Haan and P. J. T. Bussmann, *Adsorpt. Sci. Technol.*, 2006, **24**, 771–780.
- 76 M. Wang, F. Ye, H. Wang, H. Admassu, M. A. A. Gasmalla, X. Hua and R. Yang, *J. Chem. Eng.*, 2019, **370**, 1274–1285.
- 77 J. Liu, Q. Song, W. Zheng, W. Jia, H. Jia, Y. Nan, F. Ren, J. J. Bao and Y. Li, *J. Sep. Sci.*, 2022, **45**, 2415–2428.
- 78 J. C. Dore and P. C. Wankat, *Chem. Eng. Sci.*, 1976, **31**, 921–927.
- 79 M. Wang, F. Ye, H. Wang, H. Admassu, Y. Feng, X. Hua and R. Yang, *J. Agric. Food Chem.*, 2018, **66**, 9269–9281.
- 80 S. Mohapatra, N. Panda and P. Pramanik, *Mater. Sci. Eng., C*, 2009, **29**, 2254–2260.
- 81 L. Gu, Y. Wang, J. Han, L. Wang, X. Tang, C. Li and L. Ni, *New J. Chem.*, 2017, **41**, 13399–13407.
- 82 M. Glad, S. Ohlson, L. Hansson, M.-O. Månsson and K. Mosbach, *J. Chromatogr. A*, 1980, **200**, 254–260.
- 83 Z. Xu, K. M. A. Uddin, T. Kamra, J. Schnadt and L. Ye, *ACS Appl. Mater. Interfaces*, 2014, **6**, 1406–1414.
- 84 X. Zhu, J. Gu, J. Zhu, Y. Li, L. Zhao and J. Shi, *Adv. Funct. Mater.*, 2015, **25**, 3847–3854.
- 85 H. Schott, *Angew. Chem., Int. Ed. Engl.*, 1972, **11**, 824–825.
- 86 L. L. Lloyd and J. F. Kennedy, in *Process Scale Liquid Chromatography*, 1994, pp. 99–130.
- 87 D. C. Sherrington, *Chem. Commun.*, 1998, 2275–2286.
- 88 M. Berrios, J. A. Siles, M. A. Martín and A. Martín, in *Separation and Purification Technologies in Biorefineries*, 2013, pp. 149–165.
- 89 R. Rajkumar, A. Warsinke, H. Möhwald, F. W. Scheller and M. Katterle, *Talanta*, 2008, **76**, 1119–1123.
- 90 S. Schumacher, F. Grüneberger, M. Katterle, C. Hettrich, D. G. Hall, F. W. Scheller and N. Gajovic-Eichelmann, *Polymer*, 2011, **52**, 2485–2491.
- 91 H. Schmidt-Traub and A. Susanto, in *Preparative Chromatography*, 2020, pp. 525–600.
- 92 M. Yamaguchi, T. Asano, M. M. Yama and I. Iwami, *J. Food Sci.*, 1978, **43**, 1620–1621.
- 93 M. Verzele, G. Simoens and F. Van Damme, *Chromatographia*, 1987, **23**, 292–300.
- 94 S. C. Churms, *J. Chromatogr. A*, 1996, **720**, 75–91.
- 95 Y. S. Ghim and H. N. Chang, *Ind. Eng. Chem. Fundam.*, 1982, **21**, 369–374.
- 96 S. Adachi and H. Sugawara, *Arch. Biochem. Biophys.*, 1963, **100**, 468–471.
- 97 T. Xin, M. Chen, Z. Liu, R. Luo, Q. Xing, P. Bai, X. Guo and J. Lyu, *Sep. Purif. Technol.*, 2023, **319**, 124038.
- 98 C. Nobre, J. A. Teixeira and L. R. Rodrigues, *Crit. Rev. Food Sci. Nutr.*, 2015, **55**, 1444–1455.
- 99 S. J. Angyal, G. S. Bethell and R. J. Beveridge, *Carbohydr. Res.*, 1979, **73**, 9–18.
- 100 S. J. Angyal, in *Advances in Carbohydrate Chemistry and Biochemistry*, ed. R. S. Tipson and D. Horton, Academic Press, 1989, vol. 47, pp. 1–43.
- 101 J. Tiihonen, I. Markkanen and E. Paatero, *Chem. Eng. Commun.*, 2002, **189**, 995–1008.
- 102 C. Ho, C. B. Ching and D. M. Ruthven, *Ind. Eng. Chem. Res.*, 1987, **26**, 1407–1412.
- 103 J. Nowak, K. Gedicke, D. Antos, W. Piątkowski and A. Seidel-Morgenstern, *J. Chromatogr. A*, 2007, **1164**, 224–234.
- 104 A. Seidel-Morgenstern, in *Preparative Chromatography*, 2020, pp. 9–48.
- 105 H. J. Bieser and A. J. De Rosset, *Starch – Stärke*, 1977, **29**, 392–397.
- 106 Y. A. Beste, M. Lisso, G. Wozny and W. Arlt, *J. Chromatogr. A*, 2000, **868**, 169–188.
- 107 J. A. Johnson, in *Adsorption: Science and Technology*, ed. A. E. Rodrigues, M. D. LeVan and D. Tondeur, Springer Netherlands, Dordrecht, 1989, pp. 383–395.
- 108 X. Li, J. Pennington, J. F. Stobaugh and C. Schöneich, *Anal. Biochem.*, 2008, **372**, 227–236.
- 109 F. Li, X. Zhao and G. Xu, *Chin. J. Anal. Chem.*, 2006, **34**, 1366–1370.
- 110 H. Li, H. Wang, Y. Liu and Z. Liu, *Chem. Commun.*, 2012, **48**, 4115–4117.
- 111 G. Wulff, *Pure Appl. Chem.*, 1982, **54**, 2093–2102.

